energies

MDPI

Article

Techno-Economic Potential of Urban Photovoltaics: Comparison of Net Billing and Net Metering in a Mediterranean Municipality

Enrique Fuster-Palop [1], Carlos Prades-Gil [1], Ximo Masip [1], J. D. Viana-Fons [1] and Jorge Payá [2,*]

[1] Grupo ImpactE Planificación Urbana SL, Carrer Pedro Duque, Camí. de Vera s/n, 46022 Valencia, Spain; enrique.fuster@urbanimpacte.com (E.F.-P.)
[2] Instituto Universitario de Investigación en Ingeniería Energética, Universitat Politècnica de València, Camí de Vera s/n, 46022 Valencia, Spain
* Correspondence: jorge.paya@iie.upv.es

Abstract: Solar photovoltaic self-consumption is an attractive approach to increase autarky and reduce emissions in the building sector. However, a successful deployment in urban rooftops requires both accurate and low-computational-cost methods to estimate the self-consumption potential and economic feasibility, which is especially scarce in the literature on net billing schemes. In the first part of this study, a bottom-up GIS-based techno-economic model has helped compare the self-consumption potential with net metering and net billing in a Mediterranean municipality of Spain, with 3734 buildings in total. The capacity was optimized according to load profiles obtained from aggregated real measurements. Multiple load profile scenarios were assessed, revealing that the potential self-sufficiency of the municipality ranges between 21.9% and 42.5%. In the second part of the study, simplified regression-based models were developed to estimate the self-sufficiency, self-consumption, economic payback and internal rate of return at a building scale, providing nRMSE values of 3.9%, 3.1%, 10.0% and 1.5%, respectively. One of the predictors with a high correlation in the regressions is a novel coefficient that measures the alignment between the load and the hours with higher irradiance. The developed correlations can be employed for any other economic or demand scenario.

Keywords: photovoltaics; urban rooftop photovoltaic economic potential; self-consumption; self-sufficiency; net billing; regression modelling

Citation: Fuster-Palop, E.; Prades-Gil, C.; Masip, X.; Viana-Fons, J.D.; Payá, J. Techno-Economic Potential of Urban Photovoltaics: Comparison of Net Billing and Net Metering in a Mediterranean Municipality. *Energies* **2023**, *16*, 3564. https://doi.org/10.3390/en16083564

Academic Editor: Alon Kuperman

Received: 27 February 2023
Revised: 28 March 2023
Accepted: 18 April 2023
Published: 20 April 2023

1. Introduction

In recent years, photovoltaic (PV) energy has experienced a massive deployment. The European Union's (EU) total PV capacity increased from 167.5 GW in 2021 to 208.9 GW in 2022 and is expected to reach 600 GW by 2030 [1]. This rapid growth has been fostered by the consolidation of competitive manufacturing costs [2] as well as the favorable legal frameworks, policies and funds that promote the implementation of renewable systems [3]. The latter have been promoted to reduce emissions by at least 55% by 2050 in the EU [4].

Buildings in the EU are responsible for around 40% of the energy consumption and 36% of the CO_2 emissions in the zone [5]. PV self-consumption (PVSC) is a strategic approach to reach the emissions reduction target using unexploited rooftops [6]. Moreover, PVSC reduces sensitivity towards the volatility of electricity prices [7], increases independence from the grid [8] and involves citizens and other productive agents involved in the energy transition [9]. In this context, public and private agents and researchers need tools to quantify and prioritize which potential facilities on rooftops would have more impact.

For this purpose, a wide range of PV models and methodologies have been developed to assess the PV potential in urban areas [10]. Depending on the scope of the study, PV models can be classified according to their physical, geographical, technical and economic

potential [11]. Most of the literature related to the urban PV potential is circumscribed within the energy production constraints (technical potential), from the irradiance and shadow assessment to the available rooftop space or module array configurations [12,13]. In these studies, the economic dimension of the problem is out of scope due to the complexity or uncertainty of the cost scenarios [14].

As a consequence, there is scarce literature on the economic potential [14–17]. Furthermore, the applied billing scheme has a crucial influence on the feasibility results. As a relevant study in this area, Karoline Faith et al. developed a detailed GIS-based model to assess 2 km^2 of urban area in Karlsruhe (Germany) considering the economic feasibility of facilities on rooftops and façades under a net metering (NM) scheme [18]. Wider economic potential assessments with NM were applied to 55,887 buildings in Lethbridge (Canada) [19] and to the old residential buildings of five districts of Nanjing (China) [20]. Nevertheless, economic potential studies contemplating a net billing (NB) scheme are even scarcer and very few analyze nonresidential uses. To the authors' knowledge, only Jordi Olivella et al. provided a large-scale NB assessment. The latter studied 5567 real residential load profiles with a sensitivity analysis depending on the surplus reward price in London (United Kingdom) [21]. NB in contrast with NM requires the use of electricity demand curves to estimate accurately the economic savings and they vary depending on the assumptions taken on the demand profiles, as studied in the literature for specific study cases but not on a large urban scale [22,23]. In this field, the present work provides a large-scale economic PV potential sensitivity analysis by fluctuating the load profiles under an NB scheme with a bottom-up techno-economic model at a building scale. This study covers residential, industrial, and tertiary buildings, analyzing for the PV impact in a representative Mediterranean town of Spain.

In parallel, there are few proposals for agile models to reduce the computational cost in urban planning assessment. The latter would be of special interest in NB models. Simplified models based on regressions are generally employed to estimate PV production [24,25]. Some cases require complex machine-learning models [26,27]. In addition to an economic payback (*PB*) regression model proposed by the authors [28], a study case was found in which the payback and NPV model are estimated, based on installation design parameters such as power, tilt and azimuth angles, inclinations, electricity prices, among others [29]. However, both models are not very flexible to other scenarios of electricity consumption and costs. Taking advantage of the results of the PV economic potential, in the second part of this work, a methodology is proposed to develop regression-based and versatile models for different consumption and economic scenarios. For this purpose, a novel dimensionless predictor is defined to improve the correlation results. The regressions are capable of estimating energy metrics, such as self-sufficiency (*SS*) and self-consumption rate (*SC*), and economic metrics, such as *PB* and internal rate of return (*IRR*), denominated as target variables.

As a result of the previous research in the literature, the main novelties of the present work can be summarized as follows:

- NB has been compared for the first time with NM in a complete municipality. This helps to extend the impact of the results given that the regulation is different depending on the country.
- The impact of the demand profile has been studied for the first time at a municipality level under NB and NM scenarios to assess the global *SS* potential.
- Regressions have been developed for the first time to estimate *SS*, *SC*, *PB*, and *IRR*, including all the necessary parameters to implement them in a wide range of demand, costs, or price scenarios.
- A new dimensionless predictor has been introduced to address the alignment between the load and the hours with higher irradiance.
- A new optimization sizing criteria for NB has been included to guarantee high *SS* rates and low *PB*.

The article is structured as follows. Section 2 describes the techno-economic model and the scenarios, as well as the methodology to build the simplified regressions. In Section 3, the global potential results of the municipality are given, together with the impact of different load profiles on the global potential. Then, the simplified regression results are discussed, and their error metrics are calculated. Finally, in Section 3, the main conclusions are drawn.

2. Materials and Methods

Figure 1 describes the methodology that has been adopted to assess the economic potential of the municipality under an NB scheme, as well as the regressions developed to provide an agile estimation method for PV assessment in urban areas.

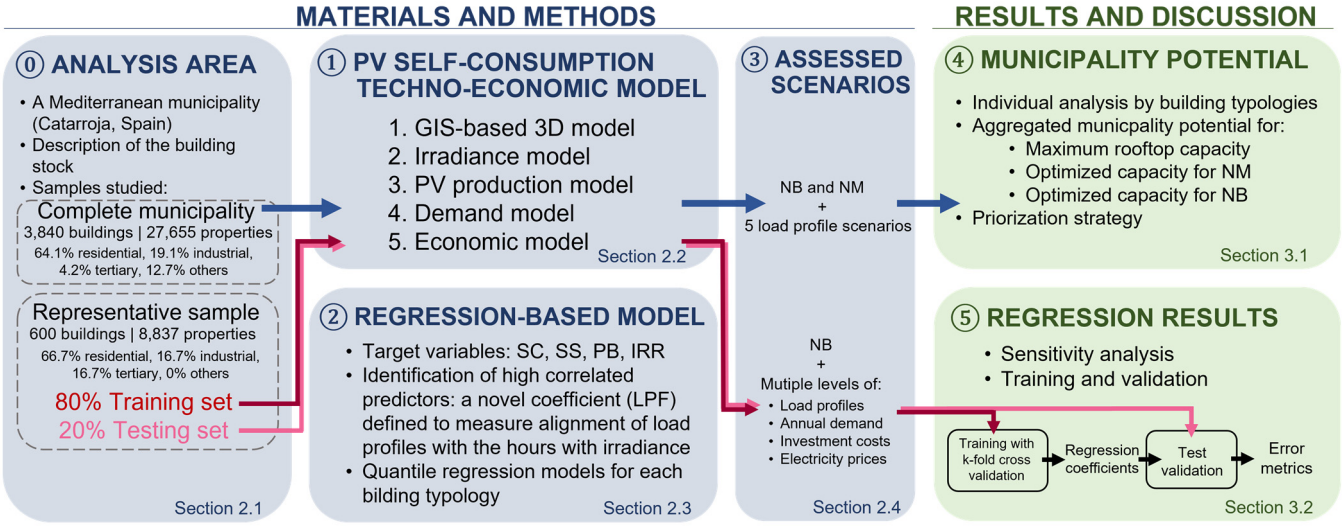

Figure 1. Methodology workflow.

First, the urban area as well as its building stock are described. Next, the techno-economic model is presented. In this section, the main assumptions, and inputs for the base case of each submodule are described with an emphasis on the demand model, which is based on real measurements. The third step presents the methodology to train and test the regressions as well as the novel predictors. Different scenarios are presented, regarding the demand, investment costs and electricity prices, as well as the different combinations of scenarios employed to train the regression-based model.

2.1. Analysis Area

The present study has been applied to the complete municipality of Catarroja, Spain (39.4028° N, 0.4044° W), which has a total extension of 13.16 km^2, and a population of 28,509 inhabitants [30]. According to the Köpen climate classification, the climate of this region is classified as Csa (hot-summer Mediterranean), with an annual global horizontal irradiation of 1782 kWh/year and an average temperature of 17.9 °C in 2021 [31] The weather conditions are similar to other European cities such as Rome (Italy), Nice (France), Athens (Greece), or Split (Croatia) [32]. The total building stock comprises 3840 independent buildings [33] that are spatially distributed according to Figure 2. The western part is an industrial park, while the eastern part is mainly the residential town center. For a more detailed PV potential analysis among buildings, the residential sector has been classified into four typologies according to the Tabula project [34], namely, single-family houses (SFHs), terrace houses (THs), multi-family houses (MFHs) and apartment blocks (ABs).

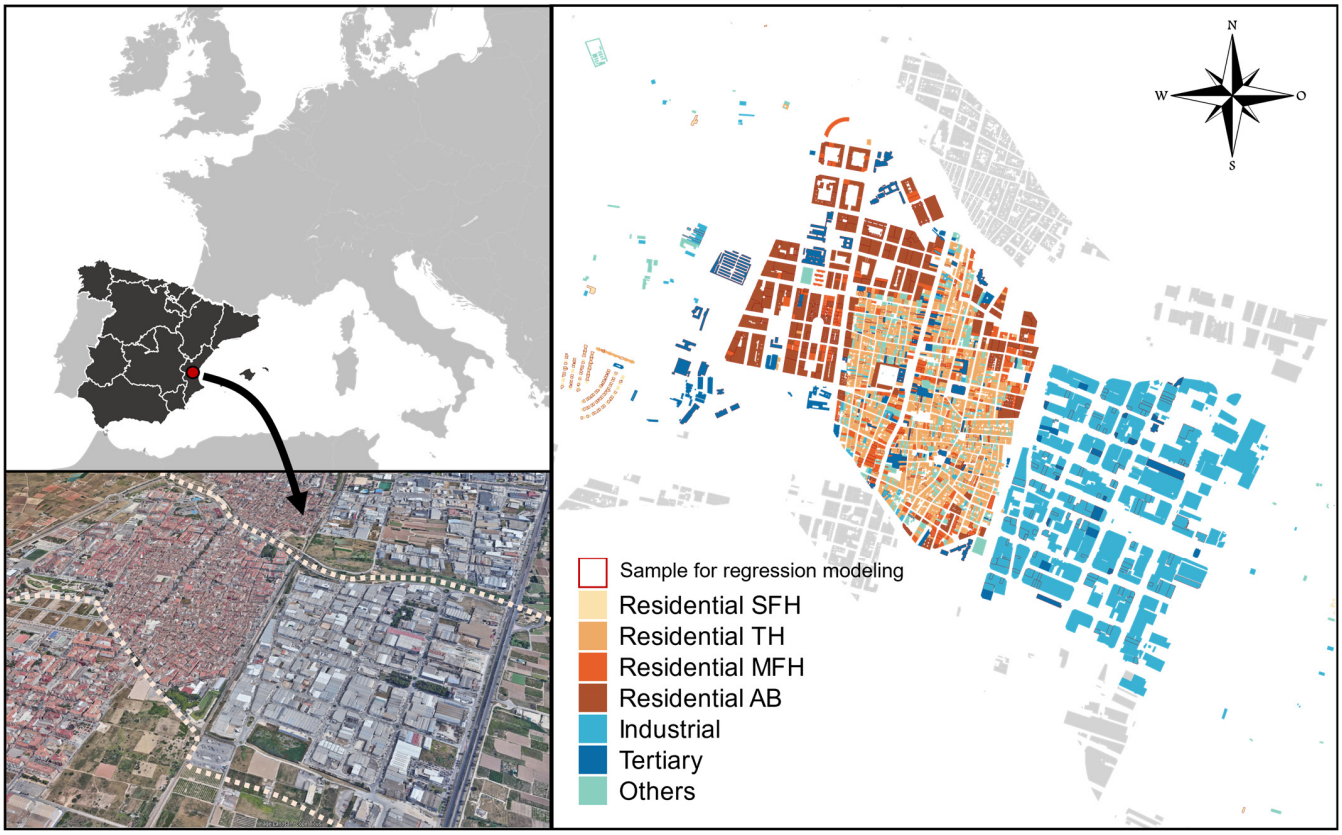

Figure 2. Geographical location and building typologies of Catarroja (Spain).

The most abundant typologies are THs. However, the largest cumulative rooftop areas are found in industrial, tertiary and ABs, as summarized in Table 1. The buildings described as *others* do not meet the Tabula classification criteria and are out of the scope of the present study given their wide range of patterns and uses.

Table 1. Building stock of the municipality of Catarroja (Spain).

Typology	Absolute Frequency	Relative Frequency	Number of Properties	Built Area	Rooftop Area
-	-	%	-	m^2	m^2
Residential SFH	132	3.44	578	23,904	14,091
Residential TH	1842	48.00	6331	451,411	206,908
Residential MFH	270	7.03	3588	345,254	76,444
Residential AB	216	5.62	13,517	1,125,487	214,148
Industrial	734	19.10	1283	504,124	462,607
Tertiary	160	4.17	794	348,652	179,230
Others	486	12.7	1564	171,407	119,613
Total	3840	100.00	27,655	2,970,239	1,273,042

For the regression modeling, a representative sample of 600 buildings Figure 2 was selected due to the high computational cost of simulating the complete municipality under the wide range of scenarios explained in Section 2.4. Six simple random samples of one hundred buildings were selected for each typology. Finally, the nonparametric Mann–Whitney U-Test [35] concluded that the difference in medians of rooftops and built areas

between the samples and the total building stock is not statistically significant for each typology, providing *p*-values above 0.25 and 0.15, respectively.

2.2. Techno-Economic Model

The bottom-up techno-economic model is composed of several submodels that allow the energy and economic performance of each rooftop facility on any building of the municipality to be obtained with the specifications provided in the present section.

The 3D GIS-based, irradiance and production model foundations are detailed in previous research by the authors. The main model hypotheses are summarized below. As a first step, a 3D GIS-based model obtains a 3D model using as main inputs the vectorial geometry of the buildings from cadaster [33] and the height of the rooftops from LiDAR data with a density of 0.5 points/m^2 [36]. The combination of GIS-based methods and LiDAR is a common and robust approach found in the literature when estimating the PV technical potential since the shadows cast by surrounding buildings reduce significantly the direct and diffuse irradiance received by the modules [10]. The model, by means of clustering techniques, helps obtain the tilt and azimuth of each surface on any rooftop, with a level of detail 2 (LoD2) in 3D models according to the CityGML standard [37]. A filter is also applied to consider a minimum rooftop area and width and to remove the small rooftop spaces [38]. For the centroid of each of the remaining surfaces, the global irradiance is applied for all combinations of azimuth and tilt using the Liu and Jordan isotropic irradiance model [39], which is widely employed in urban areas due to its accuracy and simplicity [40,41]. The shadows cast by nearby obstacles and buildings are considered to calculate the skyline of surrounding obstacles, as detailed in a previous work [28,42,43]. The irradiance hourly time-series components and ambient temperatures are obtained from PVGIS for the year 2021 [31]. The PV production is obtained through time series and the module efficiency varies with the temperature through the equation defined in reference [44]. For each surface, optimization is conducted for the tilt and azimuth angles in order to maximize the annual PV production. Specific tilt and azimuth limit angles are also considered to avoid low global efficiencies, as well as a minimum distance between panel rows. The dimensions of a commercial module are also considered in this optimization of possible configurations to avoid shadows between rows. Next, specific performance ratios and other factors are considered for the conversion from DC to AC, in agreement with experimental data [44]. As a result, the maximum AC hourly time series production and installation capacity are calculated for each facility.

Parallel to the production model, a demand model was developed to estimate the hourly electricity load curves of each dwelling or property of the municipality. One of the limitations in large-scale urban PVSC studies is the availability of real load curves to provide realistic results [45]. To reduce this gap, this model is based on measured consumption data provided by the public API of Datadis [46], as also employed in other research areas [47]. Datadis supplies the aggregated hourly electricity consumption by economic sectors (residential, industrial and services) and postal code, considering all the distributor system operators in the municipality, as well as other characteristics such as the number of contracts per sector in the postal code. This study employs the aggregated load profiles of the complete postal code (PC46470) of Catarroja. Next, the aggregated load profile of the postal code is decomposed in the following terms: (i) a dimensionless hourly time series for each economic sector normalized by its aggregated annual consumption, denominated load profile (LP). (ii) A demand scale factor (DSF) or relationship between the annual consumption and built area, calculated through Equation (1). The subscript *s*, *PC* refers to the economic sector s and postal code PC for each variable.

$$DSF_{s,PC} = \frac{D_{annual,s,PC}}{n_{contracts,s,PC}} \cdot \frac{1}{OR_{s,PC}} \cdot \frac{1}{A_{s,PC}} \quad (1)$$

The variables in Equation (1) are:

- DSF: demand scale factor.
- D_{annual}: annual demand.
- $n_{contracts}$: number of contracts. Equation (1) assumes that each dwelling or property has a single electric contract.
- OR: Occupancy rate, defined as the ratio between the inhabited properties and the total number of properties. For industrial and tertiary sectors this rate was considered 1 (full occupancy), while for the residential sector, a value of 0.81 was assumed according to the 2011 building stock census [48].
- A: average built area of each building typology, as estimated from the cadaster.

Table 2 shows the DSF obtained with Equation (1) for each economic sector in the PC studied.

Table 2. DSF values obtained through Equation (1) for each economic sector.

Economic Sector	Annual Demand	$n_{contracts}$	OR	A	DSF
-	MWh/year	-	-	m^2	kWh/m^2·year
Residential	65,839.6	24,009	0.8119	107.22	31.51
Industrial	52,247.8	760	1.0000	416.81	164.88
Tertiary	72,357.9	4401	1.0000	246.64	66.65
Unspecified	57.1	25.1	1.0000	53.54	42.52

With both variables, and the area of each dwelling ($A_{dwelling}$), which is also provided by the cadaster together with its economic sector or use, the hourly load profile of each dwelling ($D_{h,dwelling}$) of the municipality is calculated as follows in Equation (2):

$$D_{h,dwelling} = LP \cdot DSF_{s,PC} \cdot A_{dwelling} \quad (2)$$

The matching of the hourly load and production curves is performed at a dwelling level. In buildings with several independent properties that share the same PV installation, each user has been assigned a production curve proportional to the relationship between their annual demand and the aggregated annual demand of all the dwellings in the building. Even if the regulation contemplates the possibility of hourly dynamic coefficients per user to improve the energy and economic performance of facilities [49], they have been assumed to be constant throughout the year for this planning context with estimated load profiles.

The economic balance was implemented following an NB scheme, as established in the Spanish regulation (RD244/2019) [50]. The surpluses are remunerated with a lower price level than the average price of the energy term of the electricity tariff. A peculiarity of this billing scheme in Spain is that, in a given billing period (typically one month), the sum of the economic surplus remuneration cannot be higher than the economic value of the energy consumed from the grid. Thus, the user cannot perceive a negative energy term in the electricity bill at the end of the billing period. A three-period tariff scheme (2.0TD) was adopted in residential properties and a six-period scheme (3.0TD) for tertiary and industrial users, with hourly distributions found in the Spanish regulation [51]. The electricity prices shown in Table 3 are based on the average prices obtained from the operator of the Spanish electricity system [52] and an electricity supplier [53] for the 2.0TD and 3.0TD tariff, respectively, for the period between June 2021 (start of the legal application of the current tariffs schemes) and May 2022. The same period was also adopted for the price of surpluses.

Table 3. Electricity prices (€/kWh) for each tariff period.

Tariff	Period 1	Period 2	Period 3	Period 4	Period 5	Period 6
2.0TD	0.2170	0.2570	0.3221	-	-	-
3.0TD	0.2900	0.2900	0.2275	0.2035	0.1867	0.1728

To estimate the investment costs of each facility, following the method of a previous study in the same region [54], a polynomial regression (Equation (3)) was introduced to account for the economy of scale of installation costs (*IC*) of 2022 according to IVACE [55], which does not consider any subsidy.

$$IC(€) = 4.816 \cdot 10^3 + 1.084 \cdot 10^3 \cdot P_{PV} + 9.801 \cdot 10^{-2} \cdot P_{PV}^2 + 2.071 \cdot 10^{-3} \cdot P_{PV}^3 + 3.051 \cdot 10^{-6} \cdot P_{PV}^4 - 1.692 \cdot 10^{-9} \cdot P_{PV}^5 \quad (3)$$

where P_{PV} is the peak installed capacity of the facility in kW_p.

Finally, the capacity of the facility is sized according to its respective load profiles, maximizing the ratio between the global *SS* and the economic payback (*PB*) of the facility. The optimization is performed by means of the optimize function in the R package *stats* [56,57]. The model performs multiple matching iterations for different PV capacities until convergence. The maximization of the ratio *SS/PB* ensures high SS values without oversizing the facilities while keeping high profitability. The optimization of this ratio, which is novel to the best of the authors' knowledge, performs similar results as the optimization of *SC* and *SS* [58]. In addition, the proposed method represents a simplified alternative to the optimization method of technical and economic potential found in the literature [11].

As a last step, the saved emissions are obtained using an average of the national grid emission factor between 2019 and 2021.

The simulations were conducted for a lifetime period of 25 years with an hourly resolution, which is the regular standard when modeling PVSC systems in urban areas [59,60] and is sufficient to size these systems [61]. A yearly degradation in the PV modules and constant inflation and interest rates were assumed. No storage systems were considered due to their high costs [62]. The main parameters of the techno-economic model are gathered in Table 4.

Table 4. Summary of input in the base case scenario.

Parameter	Value	Units	Reference
Minimum area	5	m^2	The present study
Minimum width of the area	2	m	The present study
Minimum distance between modules	0.2	m	The present study
Maximum azimuth angle	±45	°	The present study
Maximum tilt angle	40	°	The present study
Albedo coefficient	0.2	-	[63]
Dirtiness losses	2	%	[64]
Module rated maximum power	390	kW_p	[65]
Module efficiency	20.9	%	[65]
Module width	1.052	m	[65]
Module length	1.776	m	[65]
NOCT	45	°C	[65]
Temperature coefficient of P_{max}	−0.350	%/°C	[65]

Table 4. *Cont.*

Parameter	Value	Units	Reference
Module degradation	0.816	%/year	[44]
PR	79.24	%	[44]
Surplus remuneration	0.1776	€/kWh	[52]
O&M costs	9.35	€/kW_p	[66]
Inflation rate	2	%	[67]
Interest rate	5	%	[68]
VAT	21	%	[69]
Electricity tax	5.113	%	[69]
Emissions factor	0.1593	$kgCO_2$/kWh	[70]
Facility lifetime	25	years	[71]

2.3. Regression Modeling

The target variables selected (*SS*, *SC*, *PB* and *IRR*) are those that best describe the performance of a facility in relative terms since they can be compared with other facilities regardless of their PV capacity [60]. These variables are calculated as defined in Equations (4)–(7):

$$SS(\%) = 100 \cdot \frac{SC_{annual}}{D_{annual}} \tag{4}$$

$$SS(\%) = 100 \cdot \frac{SC_{annual}}{D_{annual}} \tag{5}$$

$$PB(years) = \frac{IC}{\sum_{n=1}^{lifetime} CF_n \cdot \frac{(1+i)^{n-1}}{(1+d)^n}} \tag{6}$$

$$IRR \rightarrow NPV = 0 = \sum_{n=1}^{lifetime} \frac{CF_n}{(1+IRR)^n} \tag{7}$$

where SC_{annual} represents the annual self-consumed production, D_{annual} the annual demand, $E_{PV,annual}$ the annual PV production, i the inflation rate, d the interest rate, and CF_n the cash flows during the year n. The *IRR* is obtained by solving Equation (7) when Net Present Value (*NPV*) is 0.

As one of the aims of this article is to provide a low-cost method to estimate the economic potential in buildings with scarce information available, three potential predictor variables have been introduced, based on their correlation with the target variables:

- The load profile factor (*LPF*) is a dimensionless coefficient between 0 and 1 that measures the alignment between the load and the sun hours with more irradiance. This novel parameter is defined in Equation (8) as the cumulative sum of the product of two dimensionless time series. *LPF* is specific for each PV facility.

$$LPF = \sum_{1}^{8760} \frac{D_h}{\sum_1^{8760} D_h} \cdot \frac{I_{POA,h}}{max(I_{POA,h})|_{each\ day}} \tag{8}$$

  where:

  - D_h represents the hourly demand curve result of the aggregation of all the individual load curves of all the properties that are connected to the PV facility.
  - $I_{POA,h}$ represents the hourly global irradiance in the plane of the array.

  The first term in Equation (8) is the D_h curve normalized with respect to the annual demand and the second term is the hourly I_{POA} curve normalized with the maximum

I_{POA} of each day. With this approach, the hour of maximum production in sun hours weighs the maximum (1), and the hours of consumption in which there is no radiation weigh the minimum (0). The rest of the demands in daytime hours are weighted with a normalized production between 0 and 1. The annual cumulative sum of this product is the annual fraction of total demand consumed in conditions of the hour of peak production. This concept is similar to the capacity utilization factor of a PV installation (fraction of hours per year in which energy is produced under nominal conditions) and represents the fraction of hours per year in which electricity consumption took place under maximum production conditions. This variable could partially explain the *SS* as well as the *PB* and *IRR* under an NB scheme.

- The sizing ratio (*SR*), defined as the relationship between the peak of the load curve of the building and the peak of PV installed power, quantifies the oversizing or undersizing degree of the facility compared with the demand. Low values imply a high *SC* and a low *SS* and vice versa. Quantifying this rate is crucial in an NB scheme.
- The cost ratio (*CR*), defined as the relationship between the installation costs and the installation capacity, implicitly measures the size and economy of scale of the facility.

Additionally, to increase the flexibility and robustness towards price and costs fluctuations and other demand scenarios, three extrinsic variables were also incorporated as predictors:

- The demand level (*DL*), a rate that measures the variation in the annual demand per unit area compared with the base case scenario.
- The investment level (*IL*), a rate that quantifies the variation in the installation unit costs compared with the base case scenario.
- The price level (*PL*), a rate that measures the variation in the electricity prices of each tariff period and the surplus remuneration compared with the base case scenario.

The Ordinary Least Squares (OLS) regression constitutes a typical first approach in regression modeling [72]. However, a low degree of compliance with the OLS assumptions of linearity, normality, homoscedasticity and independent residuals and an absence of multicollinearity may lead to low confidence in the intervals inferred for the regression coefficients [73]. Due to the non-parametric nature of the distributions of the target variables obtained in the preliminary global PV potential results presented in Section 3, a quantile regression (QR) approach is proposed in this paper as an alternative to train robust models and provide more simple expressions than other nonparametric approaches such as multiadaptive regression splines. QR neither assumes normality nor homoscedasticity and is robust to outliers since the estimation is based on conditional quantile functions as a linear combination of predictors instead of mean models from OLS [74,75]. The *quantreg* R package was used to train the models [76].

Prior to the model training, the Pearson correlation coefficients are obtained to validate and select the above-defined predictors among other constructive characteristics with higher correlation with the target variables. Next, the absence of multicollinearity is checked through the variance inflation factor (VIF). As a last step in the definition of the regression formulas, multiple Box–Cox transformations [77] were applied to overcome the nonlinearity [78]. In most of the cases, the suggested exponents provided by the boxcox function of the *MASS* R package [79] were cubic and square roots. Additionally, the squared root transformation for the *PB* target variable was applied to reduce the skewness of the *PB* distribution and its linearity with the *IRR*. Finally, the building typology was included as a categorical predictor, according to the statistical differences in distributions among building typologies for the target variables detected in Section 3. As a result, six regression fits for each target variable are defined in Equations (9)–(12), where *i* represents a specific building typology

$$SS_i(\%) = f(SR, CR, LPF, DL) = \\ = k_0 + k_{0,i} + k_{1,i} \cdot \sqrt{SR} + k_{2,i} \cdot CR + k_{3,i} \cdot LPF + k_{4,i} \cdot \sqrt{LPF} + k_{5,i} \cdot DL \quad (9)$$

$$SC_i(\%) = f(SR, CR, LPF, CR, DL, SS) = \\ = k_0 + k_{0,i} + k_{1,i}\cdot SR + k_{2,i}\cdot\sqrt{SR} + k_{3,i}\cdot LPF + k_{4,i}\cdot\sqrt{LPF} + k_{5,i}\cdot\sqrt{DL} \\ + k_{6,i}\cdot SS + k_{7,i}\cdot\sqrt{SS} \quad (10)$$

$$IRR_i(\%) = f(SR, CR, LPF, DL, IL, PL, SC) = \\ = k_0 + k_{0,i} + k_{1,i}\cdot SR + k_{2,i}\cdot\sqrt{SR} + k_{3,i}\cdot CR + k_{4,i}\cdot\sqrt{CR} + k_{5,i}\cdot\sqrt[3]{CR} + k_{6,i} \\ \cdot LPF + k_{7,i}\cdot\sqrt{LPF} + k_{8,i}\cdot\sqrt[3]{LPF} + k_{9,i}\cdot DL + k_{10,i}\cdot IL + k_{11,i}\cdot PL + k_{12,i}\cdot SC \\ + k_{13,i}\cdot\sqrt{SC} + k_{14,i}\cdot\sqrt[3]{SC} \quad (11)$$

$$\frac{1}{\sqrt{PB_i}}(years^{0.5}) = f(IRR) = k_{1,i}\cdot IRR + k_{2,i}\cdot IRR^2 + k_{3,i}\cdot IRR^3 \quad (12)$$

These novel regressions constitute an improvement in the *PB* regression defined by the authors in a previous work [28], since the latter only covered facilities that occupied all the rooftop area without considering their sizing according to the load profiles.

For the training process, the results dataset obtained with the techno-economic model for each scenario defined in Table 5 was randomly split 80% into a training set and the remaining 20% into a testing set, commonly employed in the literature [72]. With the first split, a 10-fold cross-validation [44] was conducted to model each QR for each target variable. The quantile selected to predict each target variable minimizes the *RMSE* by performing a parametric calculation using quantiles between 0.05 and 0.95 with steps of 0.05.

Table 5. Simulation scenarios for the development of correlations.

Variables	Municipality Global Analysis	Regression Modeling
Sample size	Complete municipality	600 buildings
Load profile	LPA, LPB, LP0 *, LPC, LPD	LPA, LPB, LP0 *, LPC, LPD
Demand level	1.0 *	0.6, 0.8, 1.0 *, 1.2, 1.4, 1.6, 1.8
Investment level	1.0 *	0.5, 0.6, 0.7, 0.8, 0.9, 1.0 *, 1.1, 1.2
Price level	1.0 *	0.4, 0.5, 0.6, 0.7, 0.8, 0.9, 1.0 *, 1.1, 1.2
Billing scheme	NB *, NM	NB *

* Base scenario.

Finally, the testing dataset is employed to calculate the error metrics of mean absolute error (*MAE*), root mean squared error (*RMSE*), normalized root mean squared error (*nRMSE*) and the coefficient of determination (R^2), through their respective Equations (13)–(16).

$$RMSE = \sqrt{\frac{\sum_{i=1}^{N}(y_i - \hat{y}_i)^2}{N}} \quad (13)$$

$$nRMSE = \frac{\sqrt{\frac{1}{N}\sum_{i=1}^{N}(y_i - \hat{y}_i)^2}}{\bar{y_i}} \quad (14)$$

$$MAE = \frac{1}{N}\sum_{i=1}^{N}|y_i - \hat{y}_i| \quad (15)$$

$$R^2 = 1 - \frac{\sum_{i=1}^{N}(y_i - \hat{y}_i)^2}{\sum_{i=1}^{N}\left(y_i - \bar{y_i}\right)^2} \quad (16)$$

where y_i, $\hat{y}$, $\bar{y_i}$ and N are the measured, predicted and mean measured values, respectively, and N is the number of samples.

2.4. Assessed Scenarios

The PV potential of the municipality has been performed under different values of *DL*, *CL*, *PL*, load profiles and billing schemes. In addition to the base load profile obtained from Datadis for each economic sector (named henceforth as LP0), four different hourly profiles were considered for each sector (LPA, LPB, LPC and LPD), using measured profiles from several consumers in the municipality, as shown in Figure 3. The choice is based on finding different consumption patterns with the help of the values obtained for the load profile factor (*LPF*) for the global horizontal irradiance of the municipality. As a result, and according to the *LPF* values, two scenarios (LPA and LPB) have demands more aligned with high irradiance hours compared with LP0, while the other two (LPC, LPD) present more consumption during the extreme hours of the day.

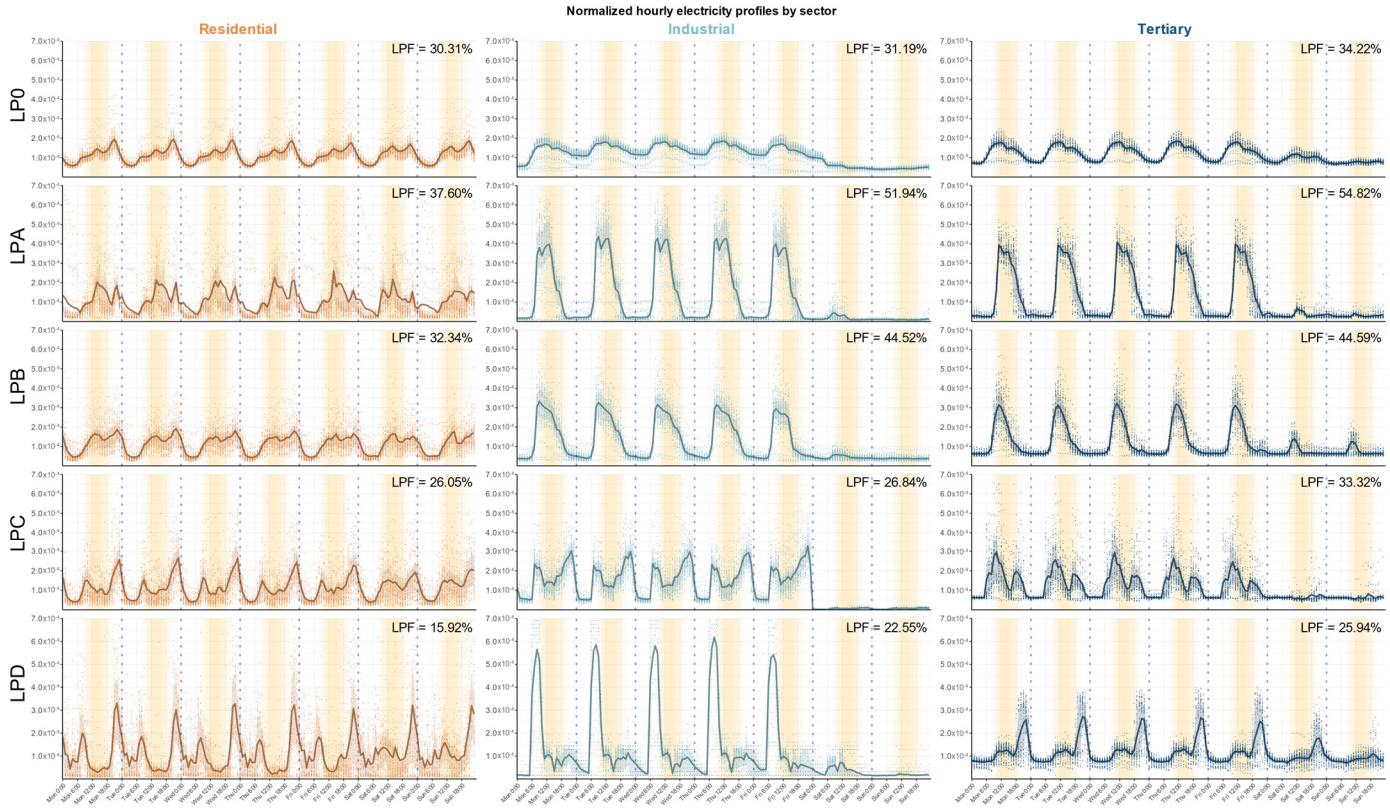

Figure 3. Normalized hourly load profiles of the assessed scenarios and their respective load profile factor.

In sum, five load profile scenarios have been studied for NB and NM schemes, respectively, as summarized in Table 5.

For the regression modeling to predict the target variables, in addition to including the above-mentioned load profiles scenarios, the variables of *DL*, *IL* and *PL* were modulated with the multiplication factors shown in Table 5. When modulating a variable, the other variables remain constant in the base scenario values.

3. Results and Discussion

This section is structured in two parts. The first part, Section 3.1, presents the results of the individual PVSC of the different building typologies, and also on an overall scale for the entire municipality. The second part, Section 3.2, shows the regression modeling results of *SS*, *SC*, *PB* and *IRR* for a representative sample of buildings in the municipality.

3.1. Municipality Self-Consumption Potential

3.1.1. Individual Results for the Different Building Typologies

For the NB base scenario, which meets the current regulatory framework in Spain, Figure 4 shows the spatial distribution of the optimized PV capacity and *PB* of each building of the municipality. While the buildings in the town center, mostly THs, require low PV capacities with higher *PB*, the opposite trend is detected in the buildings on the outskirts, which are generally industrial and MFHs. This is reflected in the bimodality of the histograms. A total of 358 buildings were not suitable for installing PV systems due to a lack of rooftop space without shadows.

Figure 5a and Table 6 show the impact of the billing scheme on the optimal sizing of PV facilities. Since surplus remuneration in NB represents approximately one-third of the regular price in the electricity tariff, the sizing optimization tends to minimize the surpluses to guarantee the profitability of each facility. In an NM scheme, the sizing tends to maximize the PV production, reaching peak powers near the maximum available on the rooftops. Despite this increase, *SS* and *SC* remain similar to the values obtained with the NB scheme. However, *SS* and *SC* of facilities with a smaller number of consumers, normally located in residential SFH and TH, are more sensitive to an increase in PV capacity, experiencing increments of 5.0%/kW_p for *SS* and 3.1%/kW_p for *SC* in contrast with the 0.9%/kW_p for *SC* and 1.0%/kW_p for *SS* of the residential AB according to their median values.

For the base case scenario, *SS* are similar among building typologies, presenting the SFHs and THs average values over 43% since the optimization tends to oversize facilities to reduce power unit costs and maximize *SS*, as seen in their low *SC* levels. This rate is similar in tertiary buildings thanks to the high *LPF* of the load profile, and higher consumers present *SS* values below 40%, mainly because of their high demand density.

The *SC* results for small residential consumers, such as TH, present an average value of 28.2%, which contrasts with the 60.1% from the residential AB. The aggregation of consumers and the rooftop space limitation allow higher *SC* rates to be obtained.

The most significant differences between NB and NM schemes are identified in the *PB* values. The highest drop in paybacks adopting an NM scenario is perceived by SFH and TH consumers. Their *PB* is reduced from 9.1 years to 5.9 and from 10.8 years to 7.1 years, respectively. The high payback values in the NB scheme are caused by higher power unit costs and a greater surpluses rate, with lower remuneration than the electricity tariff. In contrast, installations on ABs and industrial buildings, with greater economies of scale and *SC*, present average *PBs* of 3.8 and 4.2 years, respectively.

The effect of the load profile alignment with the sun hours is also gathered in Figure 5b–d and Table 7. As defined in the methodology section, the lowest *SS* rates match with the profiles with the lowest *LPF*, in this case, residential AB. In residential MFH and TH, with few dwellings and electricity consumption in the central sun hours, *SS* rates above 50% can be obtained in some cases. In MFH and AB buildings with multiple uses, the load profile aggregation tends to flatten the global demand resulting in an asymptotic growth of up to 44.2% for average SS with higher *LPF*. The highest *SS* rates are found in the tertiary and industrial sectors with averages of 52.5% and 56.8%, respectively. Regarding the lower limits, the average *SS* is over 20% for all the load profiles assessed.

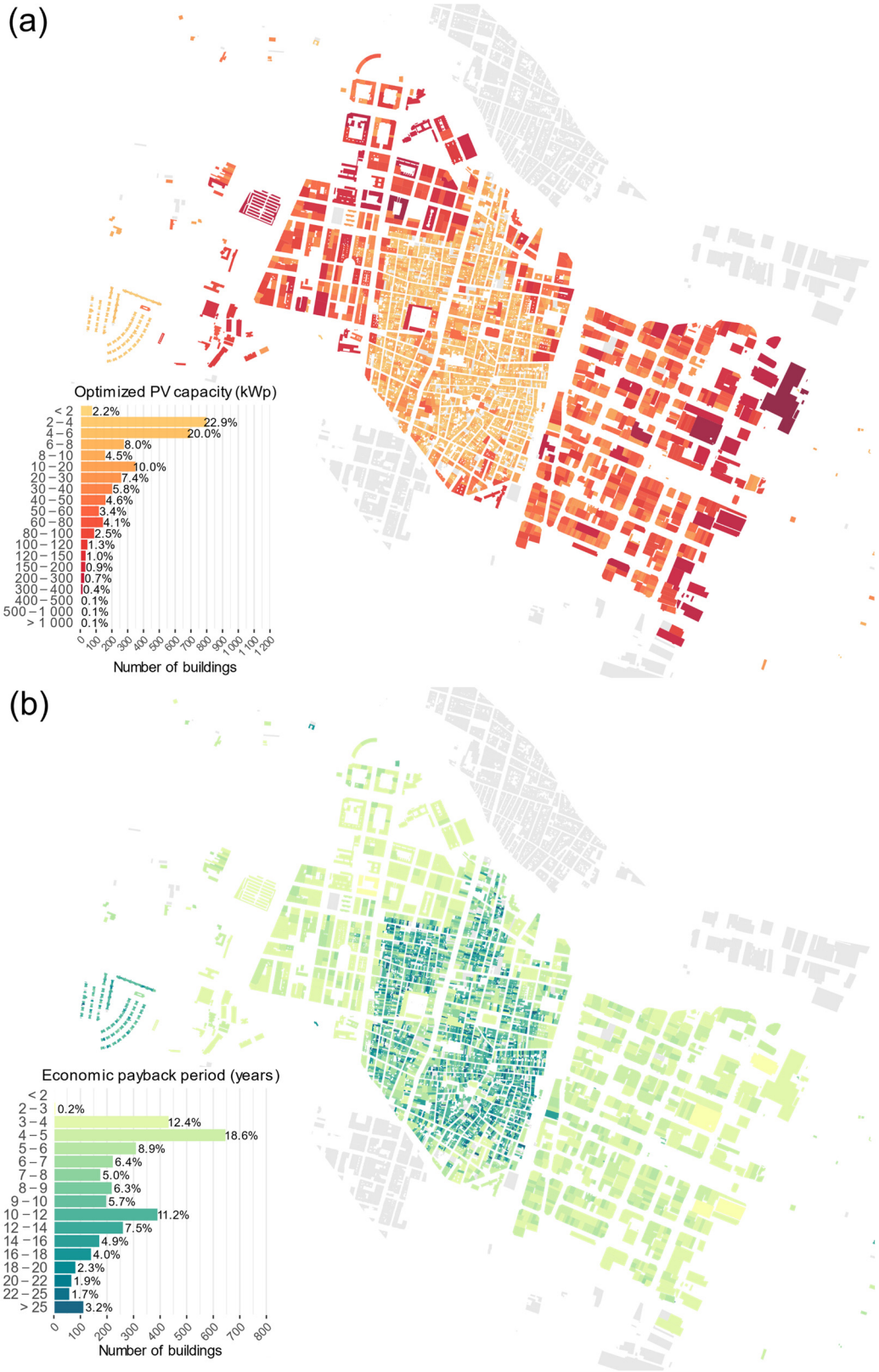

Figure 4. Spatial distribution in the municipality and histograms of (**a**) optimal capacity and (**b**) economic payback of the facilities for the base scenario.

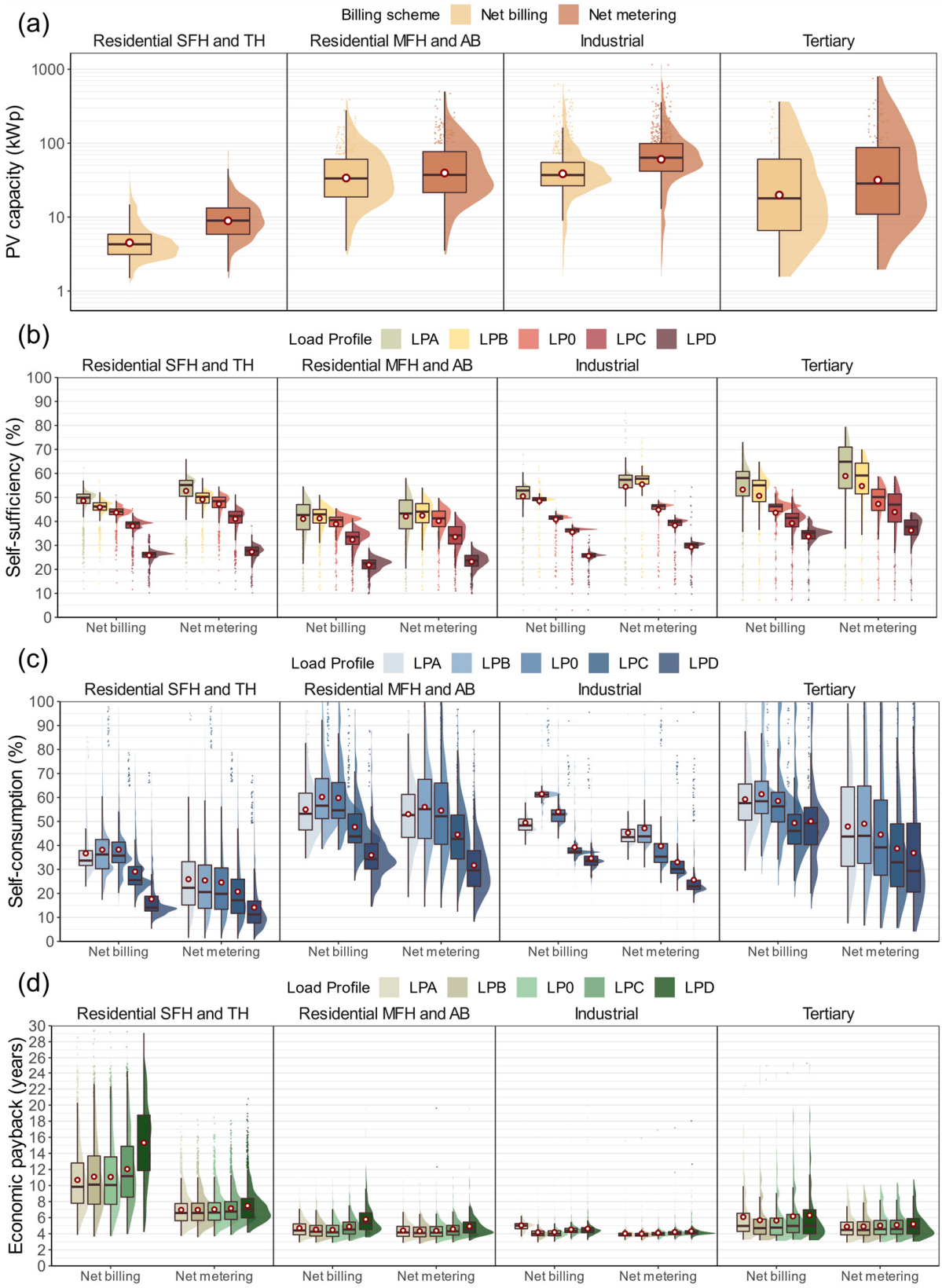

Figure 5. Boxplots of (**a**) optimal capacity of the facilities for the base scenario, and (**b**) *SS*, (**c**) *SC* and (**d**) *PB* for the different building typologies and load profiles scenarios.

Table 6. Main statistical values of PV capacity, *SS*, *SC* and *PB* by building typologies and billing scheme for the base load profile scenario.

Billing Scheme	Building Typology	Capacity *	*SS* *	*SC* *	*PB* *
-	-	kW_p	%	%	%
NB	Residential SFH	4.68/9.20	42.77/43.34	41.75/40.43	6.75/9.07
	Residential TH	4.29/5.23	44.06/43.66	35.71/38.24	9.96/10.77
	Residential MFH	20.70/23.30	40.58/38.66	54.69/59.58	4.77/5.02
	Residential AB	66.50/78.60	40.48/39.12	54.58/60.05	3.69/3.80
	Industrial	37.10/54.90	41.57/40.82	52.94/54.01	4.01/4.18
	Tertiary	17.90/48.80	46.27/43.60	56.32/58.79	4.60/5.45
NM	Residential SFH	16.80/28.60	50.36/48.83	12.24/19.31	5.31/5.85
	Residential TH	8.97/10.30	48.42/47.23	19.87/24.65	6.65/7.05
	Residential MFH	23.80/28.00	41.15/39.88	54.18/54.76	4.62/4.85
	Residential AB	77.60/95.70	41.49/40.57	51.61/54.26	3.72/3.79
	Industrial	63.60/88.60	46.39/44.83	35.30/39.70	3.96/4.11
	Tertiary	28.50/76.90	50.14/47.26	39.29/44.86	4.57/5.02

* Median/Mean.

Table 7. Main statistical values of LPA, LPB, LPC and LPD by building typologies and billing scheme for the base load profile scenario.

Variable	Building Typology	LPA *	LPB *	LP0 *	LPC *	LPD *
SS (%)	Residential SFH	48.65/48.51	52.18/51.94	46.56/46.48	40.62/40.87	27.35/27.73
	Residential TH	51.65/51.40	48.16/48.05	46.00/46.02	40.22/40.12	27.04/27.01
	Residential MFH	44.00/42.15	43.91/42.42	41.28/40.11	34.59/33.58	23.69/23.18
	Residential AB	44.00/42.15	43.91/42.42	41.06/40.42	34.59/33.58	23.69/23.18
	Industrial	54.50/52.52	51.17/52.06	42.64/42.98	37.09/36.98	27.08/27.53
	Tertiary	60.31/56.84	56.23/53.52	47.13/46.14	43.01/42.13	36.08/35.42
PB (years)	Residential SFH	5.62/5.78	5.66/5.79	5.69/5.82	5.72/5.89	5.81/6.07
	Residential TH	6.64/6.93	6.65/6.93	6.70/6.99	6.82/7.12	7.05/7.41
	Residential MFH	4.78/4.95	4.67/4.87	4.76/4.94	4.95/5.14	5.30/5.53
	Residential AB	3.76/3.85	3.73/3.81	3.79/3.86	3.92/4.02	4.20/4.32
	Industrial	3.86/4.02	3.85/3.99	3.97/4.12	4.04/4.21	4.12/4.32
	Tertiary	4.49/4.91	4.51/4.93	4.60/5.05	4.64/5.11	4.73/5.24

* Median/Mean.

For the NB scenario, the average profitability of PV facilities in all building typologies is not sensitive to the studied load profiles, especially in scenarios with equal or higher *LPF* than the base scenario. Nevertheless, residential buildings with few consumers are more sensitive to load profiles with low *LPF*. The load in these cases is mostly during the early morning, evening hours and at midnight, increasing the *PB* 38.4% for SFH (from 11.2 to 15.5 years) and 48.9% for TH (from 9.4 to 14.0 years). The other building typologies experience averaged increases in *PBs* and *IRR* below 0.5 years and −3.0%, respectively, mainly due to the concentration of consumption in the daytime hours. The fluctuations detected in the NM are mainly caused by fluctuations in the optimal PV sizing capacity compared to the NB scenario and by the different tariff periods defined in Section 2.2.

3.1.2. Aggregated Results by Building Typologies

The aggregated results for each building typology and the complete municipality and for each billing scheme are gathered in Table 8.

Table 8. Overall PV potential of the municipality.

Billing Scheme	Building Typology	PV Peak Capacity	Annual PV Production	Self-Consumption	Surpluses	Self-Sufficiency	Production-Demand ratio	Investment Costs	Economic Savings	Emission Savings
		MW_p	GWh	%	%	%	%	M€	M€/year	tCO_2/year
NB	SFH	0.25	0.34	48.53	51.47	42.02	86.58	0.43	0.08	54.11
	TH	9.96	13.45	41.32	58.68	42.01	101.66	22.41	2.99	2141.88
	MFH	6.29	8.48	57.73	42.27	37.82	65.50	9.77	2.30	1350.99
	AB	16.98	22.97	58.39	41.61	39.04	66.86	21.32	6.30	3658.92
	Industrial	40.97	56.52	53.96	46.04	40.60	75.24	49.00	13.94	9001.71
	Tertiary	7.86	10.62	67.85	32.15	23.58	34.75	9.95	2.77	1691.49
	Others	2.52	3.43	56.46	43.54	39.88	70.63	3.60	0.82	546.27
	All	84.83	115.82	54.98	45.02	37.14	67.54	116.49	29.20	18,445.36
NM	SFH	0.77	1.05	17.18	82.82	46.16	268.65	1.08	0.24	167.90
	TH	19.58	26.44	22.38	77.62	44.74	199.85	36.15	6.34	4210.84
	MFH	7.57	10.20	49.29	50.71	38.83	78.78	11.35	2.75	1624.75
	AB	20.68	27.97	49.64	50.36	40.42	81.41	25.38	7.52	4455.11
	Industrial	66.09	89.30	37.52	62.48	44.60	118.88	76.11	21.62	14,221.83
	Tertiary	12.38	16.75	45.53	54.47	24.96	54.82	14.80	4.16	2668.27
	Others	4.47	6.06	33.38	66.62	41.66	124.80	6.12	1.47	965.26
	All	131.54	177.78	38.35	61.65	39.76	103.68	171.00	44.10	28,313.97

In an ideal scenario considering all the rooftop areas of the municipality occupied by PV facilities, the maximum PV peak power installed is 145.98 MW_p, providing an annual production of 196.48 GWh, which represents 114.59% of the annual demand of the municipality. The potential annual emissions savings are 31,292 tCO_2. However, only 35.38% of the production is self-consumed and the global *SS* reaches 40.54%.

The NM scenario provides slightly lower installed capacities than the maximum power scenario. The maximum is 131.54 MW_p and the main results are shown in Table 8. The main difference is that the economic savings in this scenario yield an increase of 26.97% owing to higher surplus remuneration.

The above-mentioned values contrast significantly when considering the technical and economical limitations of an NB scenario, which is the most feasible with the current regulation. For this billing scheme, the aggregated optimal peak capacity reaches 84.33 MW_p and an annual production that represents 67.54% of the total annual demand. Despite a reduction in the maximum capacity of 57.08%, the SS rate only decreases an 8.38% and the *SC* rises to 54.98%, thereby increasing the economic profitability. With these higher rates of on-site production use, the annual economic savings would only decrease by 16.92% compared with the maximum power scenario.

Figure 6 shows the aggregated monthly municipality demand and PV production, in which the limitation of non-remunerated surpluses established by Spanish regulation is appreciated during the months with high insolation. The latter represent up to 34.3% of the total surpluses in August for the base scenario and 72.2% for the maximum power scenario. The most affected typologies by this limitation are SFHs and THs, in which up to 32.2% and 40.7% of the annual surpluses are non-remunerated, respectively. In industrial and tertiary buildings, this rate is below 10%, and for facilities shared by several consumers, the latter could be minimized with more variable sharing coefficients.

Another regulatory limiting factor to increase the production potential is the maximum allowed capacity for each facility, which is up to 100 kW_n under the regime for domestic prosumers. This is the most feasible scenario since the administrative and technical procedures are simplified. Applying this limitation and assuming a scale factor of 1.2 [64], the total capacity, *SS* and *SC* drop to 73.63 MW_p, 32.90% and 57.17%, respectively. Industrial and tertiary buildings are most affected by this limitation, with cumulative capacities falling to 34.60 MW_p, and 5.90 MW_p, respectively.

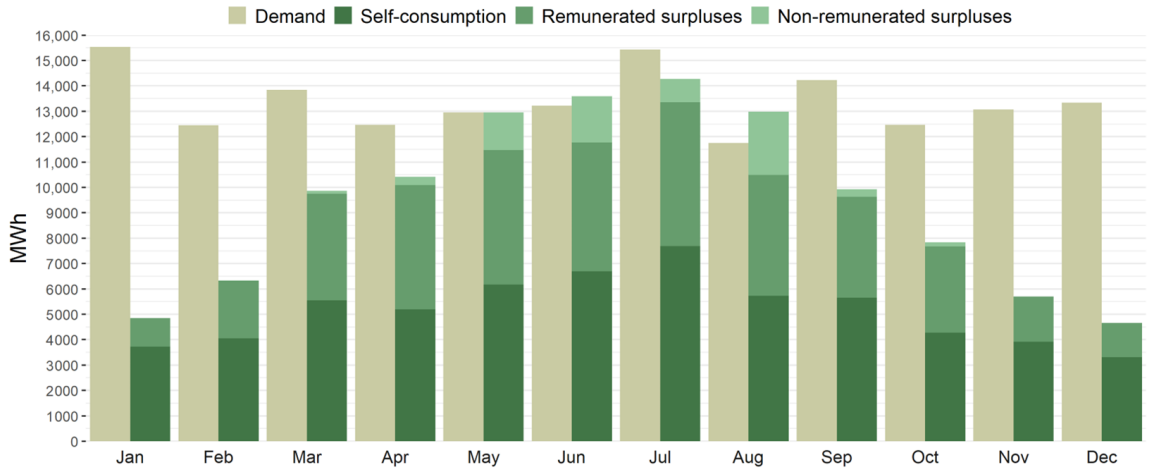

Figure 6. Monthly electricity demand and PV production for the base scenario.

If the non-profitable facilities ($IRR < 0$) for the later scenario were not installed, the final potential would drop to 73.39 MW_p. The facilities with paybacks higher than their lifetime are 24.1% of the SFHs and 21.3%.

Figure 7 reveals that high-capacity scenarios provide higher annual production than the annual demand, thereby contributing to the reduction in the emission factor from the grid. However, the global self-sufficiency barely increases compared with the NB scenarios, which require approximately half the maximum capacity.

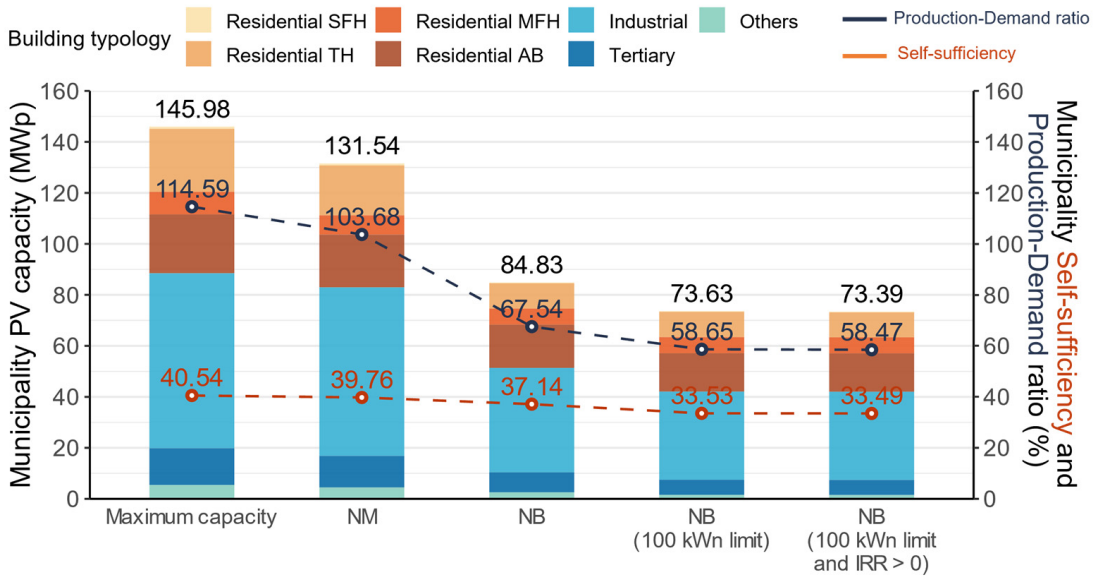

Figure 7. Comparison of aggregated capacities, self-sufficiencies and production-demand ratio for the complete municipality.

From the strategic point of view of reducing emissions, industrial building typologies provide the highest impact, followed by ABs. Both can reduce the potential emissions by 46.36% s. Figure 8 (top) shows the cumulative potential emission savings if PV facilities were installed according to different prioritization criteria. The first actions should be focused on buildings with greater demands and rooftop areas such as ABs, and industrial and tertiary buildings. Similar to the Pareto rule, by acting on 1067 buildings (90.74% AB, 87.83% industrial, 0.39% tertiary, 28.6% of the building stock municipality), 80% of the potential emission savings are reached.

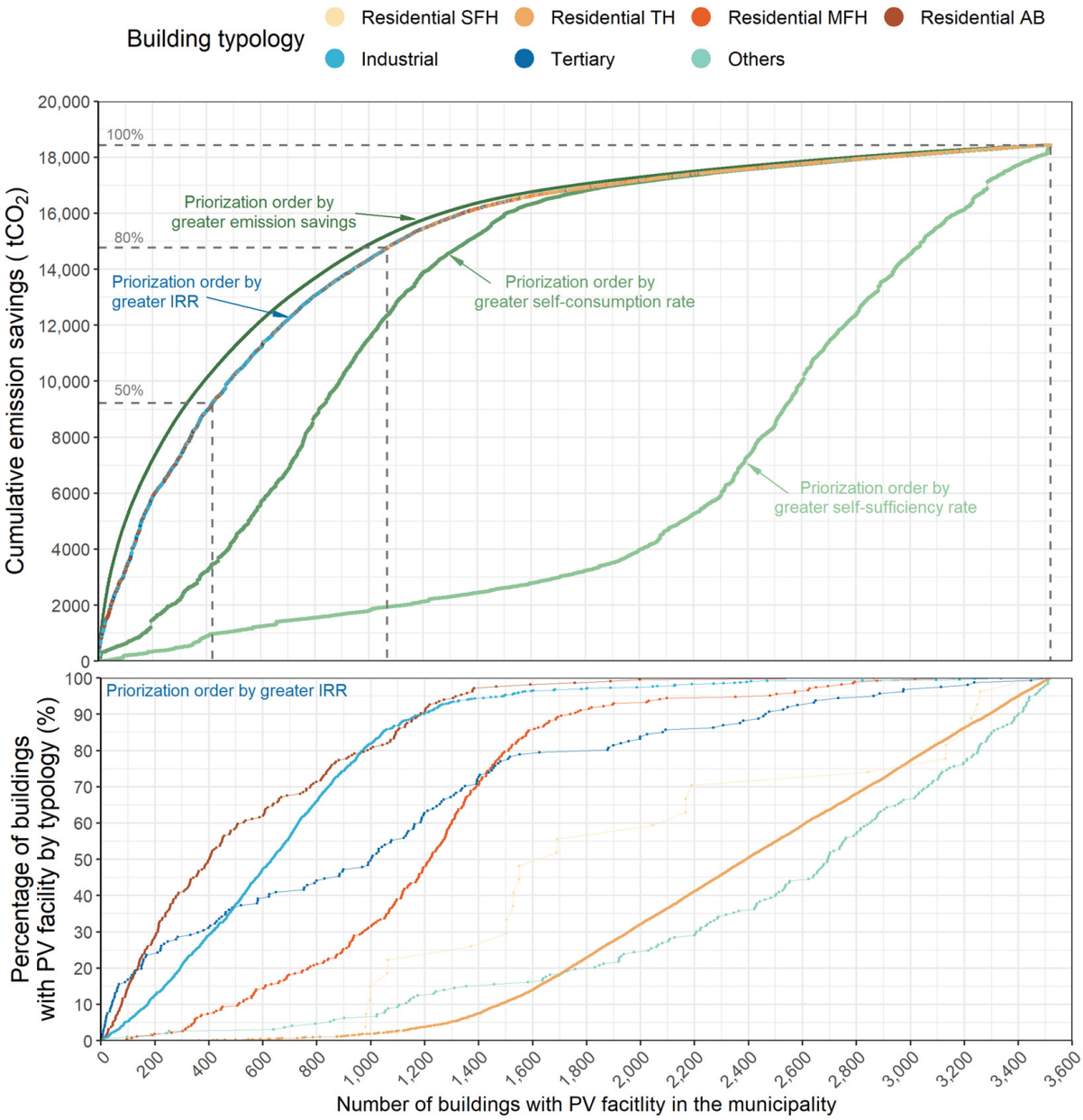

Figure 8. Cumulative potential emission savings prioritizing installations on buildings by greater *IRR*, *SC* and *SS*.

Regarding the global *SS* of the municipality, the scenarios evaluated with the different demand profiles show an asymptotic growth for the best scenario of up to 42.49%, as shown in Figure 9. This limitation is mainly caused by the presence of nighttime consumptions in all the assessed hourly profiles. Figure 9 provides a magnitude order of the error that may exist when using a given consumption profile. For the LPD scenario, which presents more nighttime consumption than the others, the *SS* is 21.93%.

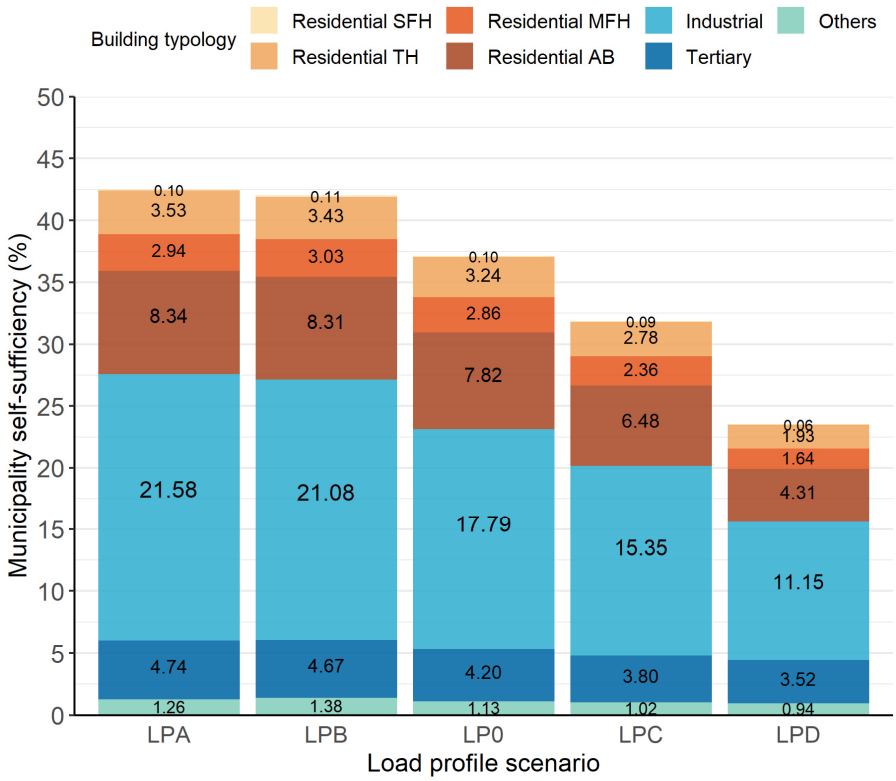

Figure 9. Contribution to the SS of the municipality of the aggregated PV production by building typology.

3.2. Regression Results

In addition to the variations assessed with the demand profiles, the global results are also conditioned by the situation of electricity prices, installation costs, and the demand level. A sensitivity analysis was performed to quantify these variations in relation to the NB base scenario and to provide a broader view of the economic feasibility of the deployment of PV systems in the municipality.

According to Figure 10 an increase in the buildings' electrification would especially benefit SFHs and THs, increasing their *SC* up to 45% and a *PB* reduction of 2.5 years with respect to the base scenario. The profitability of installations of several users of high annual demands remains practically insensitive towards these fluctuations since their *SC* rates remain high for any scenario.

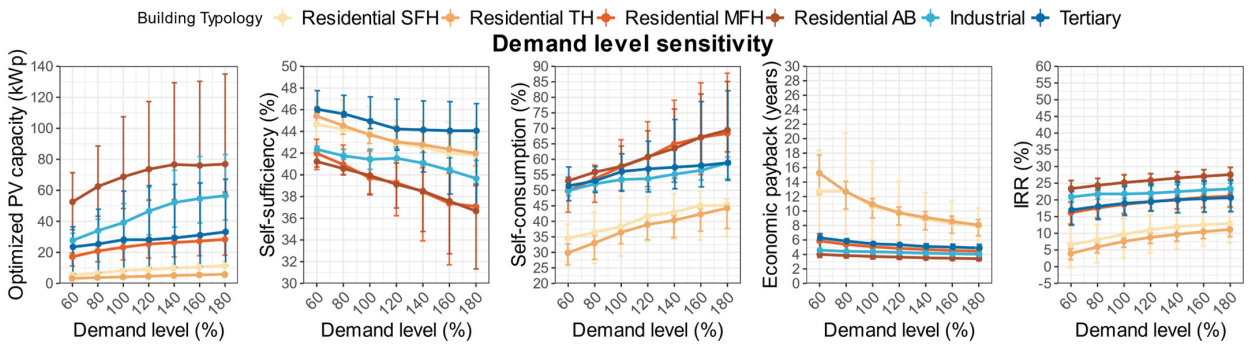

Figure 10. Sensitivity of the main PVSC variables as a function of DL with respect to the NB base scenario for the selected sample of buildings.

The variations in the results in the economic scenarios mainly affect the profitability of the facilities, as shown in Figure 11. Investment cost variations are practically linear

with *PB*, with increments for the payback for each percentual cost variation of 0.117 years for SFH and TH reaching some cases up to 20 years, while industrial or tertiary present rates around 0.05 years. Unlike investment costs, electricity price fluctuations cause similar variations in *PB*. A price scenario of 0.4 times lower than the base case scenario, which is representative of the first half of 2021 in Spain, would increase the average PBs up to 26.5 years for SFHs, 12.0 years for ABs and 14.4 years for industrial buildings.

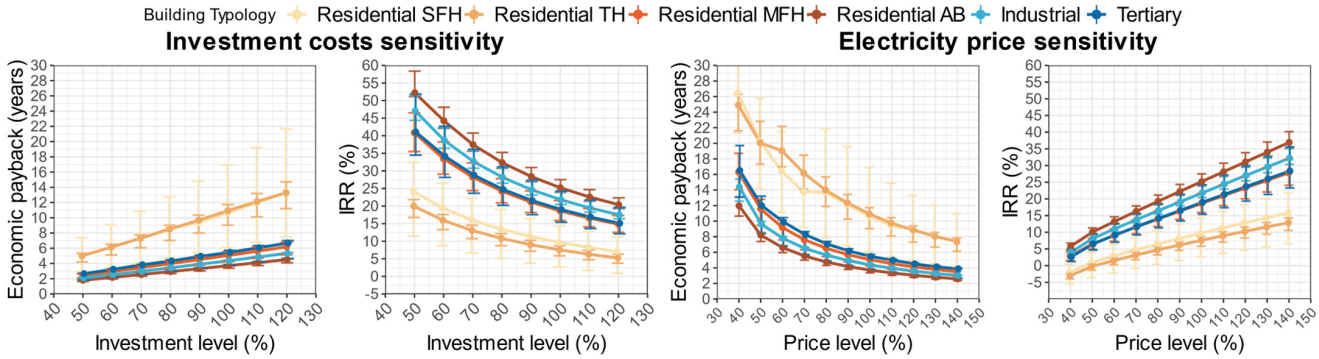

Figure 11. Sensitivity of the main PVSC variables as a function of investment CL and PL with respect to the NB base scenario for the selected sample of buildings.

With the results of the sample of buildings, the Pearson correlation matrix in Figure 12 helps identify the most explanatory variables to predict the *SS*, *SC*, *PB* and *IRR* using QR models. Among the preliminary predictors, the constructive characteristics of buildings such as height, rooftop area and dwellings area were discarded due to their low correlation values with the target variables. Furthermore, their information is partially included in the other predictors. As mentioned in Section 2.3, the predictors selected for the final models are the following: *SR*, *CR*, *LPF*, *DL*, *IL* and *PL*.

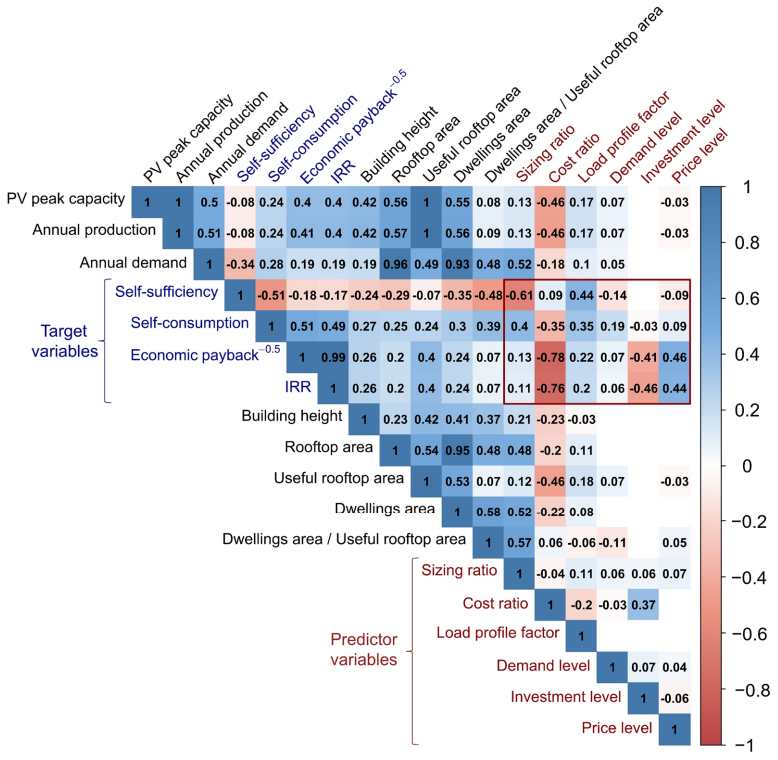

Figure 12. Correlation matrix of the main PVSC variables, physical characteristics of the buildings and assessed techno-economic scenarios.

The correlation matrix values provide an intuitive idea about the workflow proposed in the training of the regressions. As a first step, *SS* is predicted thanks to the high correlation with the SR and the LPF, which are less correlated with the other target variables. Next, the predicted *SS* is used as a reinforcement predictor of *SC*. Lastly, the economic target variables (*PB* and *IRR*) present a low correlation with the two intrinsic predictors (SR and *LPF*), which potentially leads to mispredictions due to scarce differentiation among individuals. To reduce the errors in the economic regressions, the *SC* variable is also employed as a predictor with a moderate correlation. The multicollinearity, measured with the VIF, is lower than 2 for all of them, except for a VIF of 7.1 between cost ratio and investment level to predict the *IRR*.

The relationship between the two main predictors for *SS* is shown in Figure 13. Each point represents a result for a specific building. The *LPF* provides a clear positive correlation with *SS*, however, this variable only considers the alignment of consumption with sun hours and no other effects such as how a facility is undersized compared with its load. The latter aspect is expressed with the sizing factor (relationship between the peak demand and peak PV capacity).

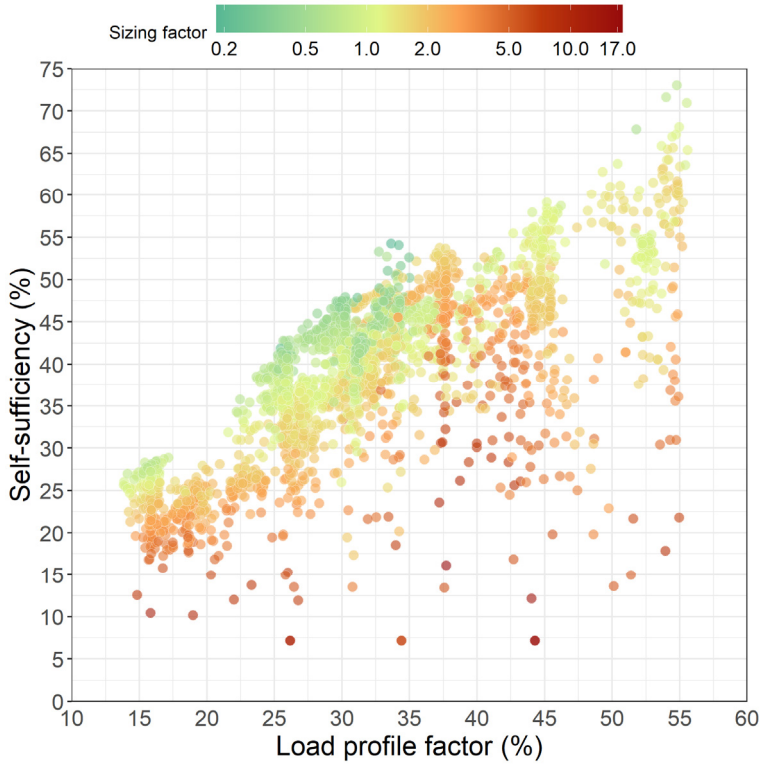

Figure 13. Scatter plot of *SS* and its main predictor variables (load profile factor and sizing factor).

The QR expressions are defined in Section 2.3 and the values of the fitted coefficients for each variable and building typology are described in Appendix A.

Figure 14 compares the calculated target variables through the techno-economic model and the prediction from each regression model. The greater relative errors are found in the overpredictions in the economic variables with less profitable facilities. This is partially caused by an overprediction of the *SS* regression model for big consumers, for which the optimal capacity is limited by the available rooftop space. This non-linearity, for instance, causes differences in accuracy between ABs (84.00%) or Tertiary (90.53%) and SFHs (98.44%) or THs (96.83%).

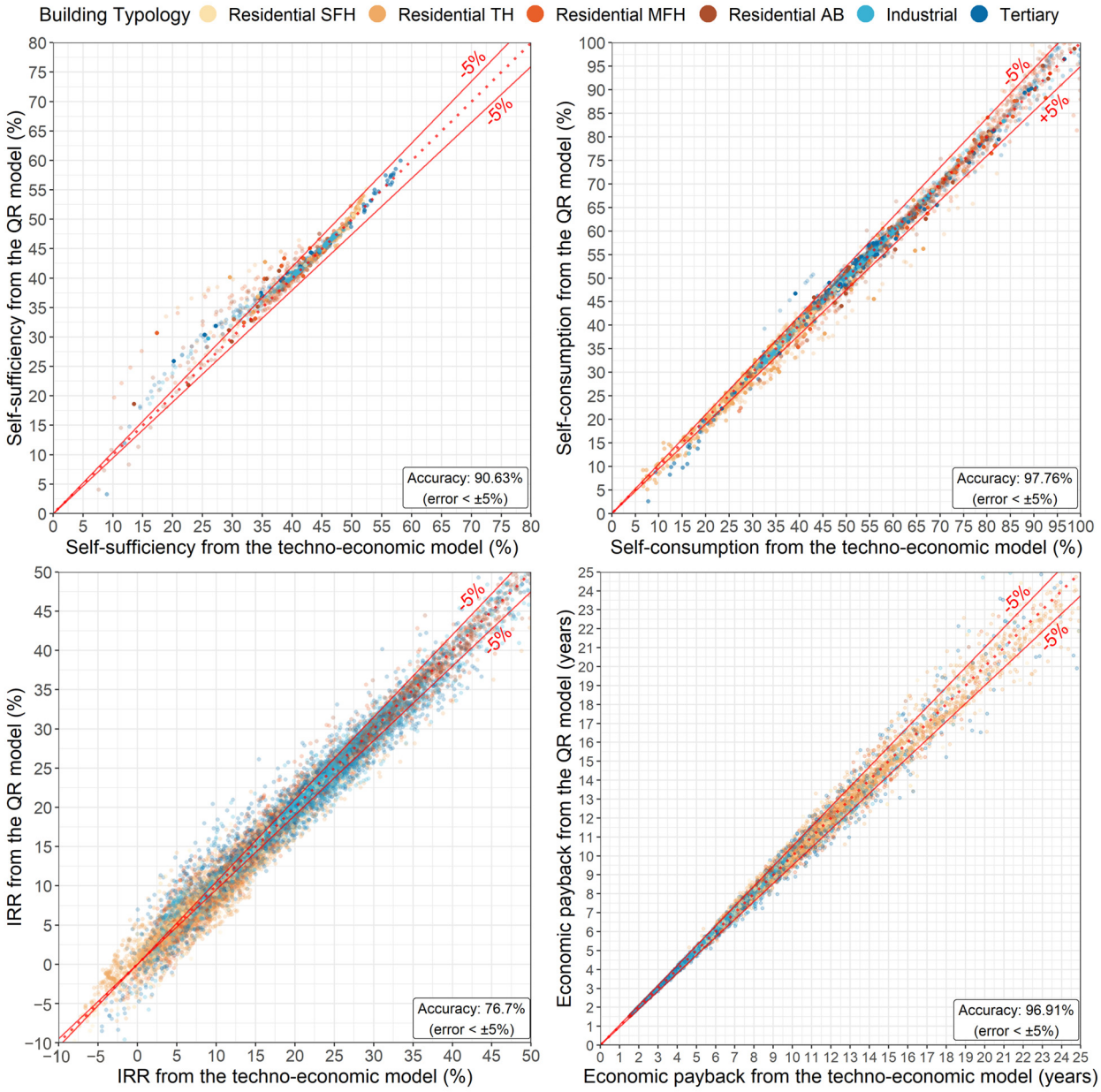

Figure 14. Validation of the predicted values *SS*, *SC*, *IRR* and *PB* by the QR models.

Finally, the main error metrics of each model are gathered in Table 9. The *nRMSEs* of *SS* and *SC* are below 4%, and of *PB* is below 2%, which are reasonable for planning purposes.

Table 9. Error metrics of the predicted *SS*, *SC*, *IRR* and *PB* by the QR models.

Target Variable	*MAE*	*RMSE*	*nRMSE*	R^2
SC	0.805%	1.627%	3.866%	0.911
SS	0.831%	1.536%	3.097%	0.992
IRR	0.012%	0.018%	10.020%	0.974
PB	0.015 years	0.023 years	1.479%	0.997

4. Conclusions

Currently, there are few studies in the literature on the economic assessment of PVSC facilities on an urban scale for NB schemes. In the present work, a bottom-up techno-economic model was developed to estimate hourly load profiles at a property level. In

the first part of this paper, the techno-economic potential was evaluated for the complete building stock of 3840 buildings in the Mediterranean municipality of Catarroja, Spain. Different hourly load profiles were analyzed and compared within the NM scenario.

According to the electricity prices between 2021 and 2022, and based on the present legal framework in Spain, the average payback is 9–10 years for SFHs and THs, while MFHs, Industrial and Tertiary building typologies yield paybacks of 4–5 years. The most feasible facilities are placed on ABs owing to their high number of consumers and scarce surpluses. Except for SFHs and THs, the other building typologies yield nevertheless very similar paybacks with the NM scheme.

Regarding the variation in load profiles, for the scenarios with the lowest *LPF*, the *PB* of facilities on SFHs and THs experiences on average an increase of around 5 years, while buildings with higher demands are not sensitive to these fluctuations. The highest *SS* are found in facilities on Tertiary buildings for the highest LPF, reaching on average up to 67.6%, while residential typologies barely surpass the *SS* values of 50%.

For the aggregated balance of the municipality, there is a wide difference between the total capacity under NM and NB schemes, with 131.54 MW_p and 84.83 MW_p, respectively. This reduction shows the importance of considering the economic constraints when estimating the urban PV potential of any city under the NB regulation. Under the NB scheme, the total *SS* of the municipality fluctuates between 42.5% for the highest *LPF* scenario and 21.9% for the lowest. However, the total PV energy produced would represent 67.5% of the total electricity consumption of the municipality. This rate could rise to 103.7% with an NM scheme. For the municipality energy strategy, prioritizing PV facilities on 28.6% of the most economically feasible rooftops would deliver 80% of the potential emission savings due to electricity consumption. The most relevant typologies in this process are those with high consumption and high rooftops such as ABs and industrial buildings.

As a second part of this work, four QR models were developed to predict *SS*, *SC*, *PB* and *IRR* through the intrinsic characteristics of the installations as well as other conjunctural characteristics such as demand, prices, or cost variations. One of the predictors defined is the LPF, a novel coefficient that addresses the alignment of the building consumption and the PV production, which is one of the main explanatory variables to predict the *SS*. The cost ratio, which measures the economy of scale of the facility, is a significant predictor to estimate the economic target variables. The models provide estimations for the above-mentioned variables with *nRMSE* values of 3.9%, 3.1%, 10.0% and 1.5%, respectively, compared with the techno-economic model.

The most relevant outcomes are:

- The sizing of the facilities according to the load curves in the NB modality, optimizing *SS* and profitability, is crucial to obtain competitive economic returns while maintaining similar levels of *SS* with those obtained in NM.
- SFHs and THs are the most sensitive to the shape of the hourly load profile. More detailed approaches are required in residential areas to estimate load profiles of SFHs and THs.
- Considering the profitability constraints under the current NB scheme, the total neutrality of emissions of municipal electricity consumption would not be achieved by the deployment of rooftop PVSC systems, in contrast to the NM scheme.
- The best economic and environmental results are achieved with ABs, industrial and tertiary buildings.
- The *LPF* is a crucial predictor to estimate *SS* and *SC* through regression-based models for the NB in which there is not a direct relationship between these variables and other constructive aspects of the building.

Author Contributions: Conceptualization, E.F.-P. and J.P.; methodology, E.F.-P., C.P.-G., J.D.V.-F. and J.P.; software, E.F.-P. and J.D.V.-F.; validation, E.F.-P., J.P. and J.D.V.-F.; formal analysis, E.F.-P.; investigation, E.F.-P.; resources, C.P.-G., X.M. and J.D.V.-F.; data curation, E.F.-P.; writing—original draft preparation, E.F.-P.; writing—review and editing, E.F.-P. and J.P.; visualization, E.F.-P.; supervision,

J.P.; project administration, J.P.; funding acquisition, C.P.-G. and X.M. All authors have read and agreed to the published version of the manuscript.

Funding: This research received no external funding.

Data Availability Statement: Not applicable.

Acknowledgments: The authors would like to thank the City Council of Catarroja and Grupo ImpactE Planificación Urbana S.L for supporting this project.

Conflicts of Interest: The authors declare no conflict of interest.

Nomenclature

€	Euro
3D	Three-dimensional
A	Area
AB	Apartment block
CO_2	Carbon dioxide
CF	Cash flow
CR	Cost ratio
d	Interest rate
D_{annual}	Annual demand
D_h	Hourly demand
DL	Demand level
DSF	Demand scale factor
E_{PV}	Annual photovoltaic production
Eq	Equation
GIS	Geographic Information System
GWh	Gigawatt hour
I	Inflation rate
IC	Installation costs
IL	Investment level
IPOA	Global irradiance in the plane of array
IRR	Internal rate of return
kg	kilogram
kWh	Kilowatt-hour
kW_n	Nominal kilowatt
kW_p	kilowatt peak
LiDAR	Light Detection and Ranging
LoD	Level of detail
LP	Load profile
m	Linear meter
M€	Millions of Euros
m^2	Square meter
MAE	Mean absolute error
MFH	Multi-family house
MW_p	Megawatt peak
$n_{contracts}$	Number of contracts
NB	Net billing
NM	Net metering
NPV	Net present value
nRMSE	Normalized root mean squared error
$^{\circ}C$	Degrees Celsius
OLS	Ordinary Least Squares

OR	Occupation rate
P_{PV}	PV peak capacity
PB	Economic payback
PC	Postal code
PL	Price level
PV	Photovoltaic
QR	Quantile regression
R^2	Coefficient of determination
RD	Royal decree
RMSE	Root mean squared error
SC	Percentage of Self-consumption
SC_{annual}	Annual self-consumed energy
SFH	Single-family house
SR	Sizing ratio
SS	Self-sufficiency
t	Tonne
TH	Terrace house
VIF	Variance inflation factor

Appendix A

Table A1. QR coefficients to estimate *SS* for each building typology.

Building Typology	Coefficient	Value	95% CI	*p*-Value
-	k_0 (Intercept)	−13.46	−246.1; 219.2	>0.910
Residential SFH	k_0 (Intercept)	-	-	-
	k_1 ($SR^{0.5}$)	−17.69	−19.01; −16.37	0.000
	k_2 (LPF)	−114.11	−877.9; 649.7	0.770
	k_3 ($LPF^{0.5}$)	194.00	−648.2; 1036	0.652
	k_4 ($DL^{0.5}$)	−0.41	−0.809; −0.004	0.048
Residential TH	k_0 (Intercept)	−280.88	−513.9; −47.84	0.018
	k_1 ($SR^{0.5}$)	−19.15	−19.18; −19.12	<0.001
	k_2 (LPF)	−1092.27	−1139; −1046	<0.001
	k_3 ($LPF^{0.5}$)	1243.85	1193; 1294	<0.001
	k_4 ($DL^{0.5}$)	−0.06	−0.149; 0.021	0.139
Residential MFH	k_0 (Intercept)	−930.61	−1271; −590.6	<0.001
	k_1 ($SR^{0.5}$)	−23.24	−23.57; −22.91	<0.001
	k_2 (LPF)	−3391.60	−4198; −2586	<0.001
	k_3 ($LPF^{0.5}$)	3696.59	2802; 4591	<0.001
	k_4 ($DL^{0.5}$)	−0.22	−0.652; 0.203	0.304
Residential AB	k_0 (Intercept)	2540.30	2235; 2846	<0.001
	k_1 ($SR^{0.5}$)	−21.47	−21.79; −21.15	<0.001
	k_2 (LPF)	7839.67	7204; 8476	<0.001
	k_3 ($LPF^{0.5}$)	−8793.75	−9504; −8084	<0.001
	k_4 ($DL^{0.5}$)	−0.51	−0.822; −0.197	0.001
Industrial	k_0 (Intercept)	198.66	−182.0; 579.3	0.306
	k_1 ($SR^{0.5}$)	−28.85	−28.99; −28.72	<0.001
	k_2 (LPF)	563.56	−416.1; 1543	0.260
	k_3 ($LPF^{0.5}$)	−533.48	−1620; 553.1	0.336
	k_4 ($DL^{0.5}$)	−0.66	−0.732; −0.580	<0.001
Tertiary	k_0 (Intercept)	−7.95	−525.0; 509.1	0.976
	k_1 ($SR^{0.5}$)	−28.75	−29.30; −28.20	<0.001
	k_2 (LPF)	−16.96	−1389; 1355	0.981
	k_3 ($LPF^{0.5}$)	162.53	−1430; 1755	0.841
	k_4 ($DL^{0.5}$)	−0.37	−0.628; −0.119	0.004

Table A2. QR coefficients to estimate *SC* for each building typology.

Building Typology	Coefficient	Value	95% CI	*p*-Value
-	k_0 (Intercept)	−564.71	−1599.58; 470.15	0.285
Residential SFH	k_0 (Intercept)	-	-	-
	k_0 (SR)	39.68	14.08; 65.27	0.002
	k_2 ($SR^{0.5}$)	−3.87	−35.46; 27.71	0.810
	k_3 (LPF)	860.61	−3992.07; 5713.29	0.728
	k_4 ($LPF^{0.5}$)	−842.09	−6153.69; 4469.51	0.756
	k_5 ($DL^{0.5}$)	0.02	−0.39; 0.43	0.925
	k_6 (SS)	−19.25	−37.08; −1.41	0.034
	k_7 ($SS^{0.5}$)	245.64	2.63; 488.65	0.048
Residential TH	k_0 (Intercept)	2490.66	1441.75; 3539.57	<0.001
	k_0 (SR)	4.58	0.02; 9.14	0.049
	k_2 ($SR^{0.5}$)	22.39	14.59; 30.18	<0.001
	k_3 (LPF)	6521.00	6046.98; 6995.01	<0.001
	k_4 ($LPF^{0.5}$)	−6832.29	−7343.48; −6321.11	<0.001
	k_5 ($DL^{0.5}$)	0.12	0.03; 0.21	0.012
	k_6 (SS)	−1.72	−4.36; 0.91	0.200
	k_7 ($SS^{0.5}$)	−7.29	−41.59; 27	0.677
Residential MFH	k_0 (Intercept)	3593.36	2551.86; 4634.86	<0.001
	k_0 (SR)	10.71	9.5; 11.92	<0.001
	k_2 ($SR^{0.5}$)	−7.80	−10.39; −5.21	<0.001
	k_3 (LPF)	11,761.48	11,367.87; 12,155.1	<0.001
	k_4 ($LPF^{0.5}$)	−12,320.11	−12,749.3; −11,890.93	<0.001
	k_5 ($DL^{0.5}$)	−0.25	−0.35; −0.14	<0.001
	k_6 (SS)	−12.35	−12.57; −12.13	<0.001
	k_7 ($SS^{0.5}$)	116.26	113.61; 118.9	<0.001
Residential AB	k_0 (Intercept)	6224.83	4405.08; 8044.57	<0.001
	k_0 (SR)	8.18	5.07; 11.28	<0.001
	k_2 ($SR^{0.5}$)	−3.81	−9.61; 2	0.198
	k_3 (LPF)	20,214.43	15,382.25; 25,046.61	<0.001
	k_4 ($LPF^{0.5}$)	−21,747.05	−27,132.16; −16,361.93	<0.001
	k_5 ($DL^{0.5}$)	−0.27	−0.35; −0.18	<0.001
	k_6 (SS)	−12.40	−13.15; −11.65	<0.001
	k_7 ($SS^{0.5}$)	115.80	106.5; 125.1	<0.001
Industrial	k_0 (Intercept)	3008.01	1956.49; 4059.53	<0.001
	k_0 (SR)	−8.29	−10.44; −6.14	<0.001
	k_2 ($SR^{0.5}$)	48.38	45.11; 51.65	<0.001
	k_3 (LPF)	9127.51	8520.73; 9734.29	<0.001
	k_4 ($LPF^{0.5}$)	−9758.73	−10,442.43; −9075.04	<0.001
	k_5 ($DL^{0.5}$)	0.15	0.1; 0.2	<0.001
	k_6 (SS)	−8.76	−8.99; −8.52	<0.001
	k_7 ($SS^{0.5}$)	84.59	81.63; 87.56	<0.001
Tertiary	k_0 (Intercept)	−2930.08	−4111.86; −1748.29	<0.001
	k_1 (SR)	5.75	−5.55; 17.05	0.319
	k_2 ($SR^{0.5}$)	45.51	34.17; 56.84	<0.001
	k_3 (LPF)	−8977.73	−10,751.11; −7204.36	<0.001
	k_4 ($LPF^{0.5}$)	10,741.19	8664.91; 12,817.48	<0.001
	k_5 ($DL^{0.5}$)	−0.06	−0.19; 0.08	0.396
	k_6 (SS)	−10.24	−11.31; −9.17	<0.001
	k_7 ($SS^{0.5}$)	114.37	97.94; 130.8	<0.001

Table A3. QR coefficients to estimate *IRR* for each building typology.

Building Typology	Coefficient	Value	95% CI	*p*-Value
-	k_0 (Intercept)	−2.94	−16.14; 10.27	0.663
Residential SFH	k_0 (Intercept)	0.01	−0.16; 0.19	0.891
	k_1 (SR)	0.00	−0.38; 0.37	0.981
	k_2 ($SR^{0.5}$)	0.00	0; 0	<0.001
	k_3 (CR)	0.34	0.19; 0.49	<0.001
	k_4 ($CR^{0.5}$)	−1.50	−2.12; −0.88	<0.001
	k_5 ($CR^{1/3}$)	11.62	−15.78; 39.03	0.406
	k_6 (LPF)	−57.63	−165.6; 50.34	0.295
	k_7 ($LPF^{0.5}$)	54.73	−40.9; 150.37	0.262
	k_8 ($LPF^{1/3}$)	0.00	−0.01; 0	0.889
	k_9 (DL)	0.02	0.01; 0.04	0.001
	k_{10} (IL)	0.17	0.16; 0.17	<0.001
	k_{11} (PL)	−0.01	−0.02; 0	0.135
	k_{12} (SC)	0.43	0.09; 0.77	0.012
	k_{13} ($SC^{0.5}$)	−0.87	−1.45; −0.28	0.004
	k_{14} ($SC^{1/3}$)	0.01	−0.16; 0.19	0.891
Residential TH	k_0 (Intercept)	15.71	0.49; 30.93	0.043
	k_1 (SR)	−0.01	−0.02; −0.01	0.001
	k_2 ($SR^{0.5}$)	0.05	0.03; 0.07	<0.001
	k_3 (CR)	0.00	0; 0	<0.001
	k_4 ($CR^{0.5}$)	0.24	0.19; 0.29	<0.001
	k_5 ($CR^{1/3}$)	−1.08	−1.29; −0.87	<0.001
	k_6 (LPF)	−19.43	−35.27; −3.59	0.016
	k_7 ($LPF^{0.5}$)	72.46	10.33; 134.58	0.022
	k_8 ($LPF^{1/3}$)	−62.69	−117.65; −7.73	0.025
	k_9 (DL)	0.00	0; 0.01	0.008
	k_{10} (IL)	0.04	0.03; 0.05	<0.001
	k_{11} (PL)	0.14	0.14; 0.14	<0.001
	k_{12} (SC)	−0.01	−0.01; −0.01	<0.001
	k_{13} ($SC^{0.5}$)	0.59	0.46; 0.73	<0.001
	k_{14} ($SC^{1/3}$)	−1.21	−1.49; −0.94	<0.001
Residential MFH	k_0 (Intercept)	4.67	−8.7; 18.04	0.494
	k_1 (SR)	0.01	0.01; 0.01	<0.001
	k_2 ($SR^{0.5}$)	−0.03	−0.04; −0.02	<0.001
	k_3 (CR)	0.00	0; 0	<0.001
	k_4 ($CR^{0.5}$)	0.45	0.39; 0.51	<0.001
	k_5 ($CR^{1/3}$)	−1.91	−2.12; −1.7	<0.001
	k_6 (LPF)	10.36	6.75; 13.97	<0.001
	k_7 ($LPF^{0.5}$)	−46.98	−62.27; −31.7	<0.001
	k_8 ($LPF^{1/3}$)	43.57	29.69; 57.45	<0.001
	k_9 (DL)	0.00	0; 0	<0.001
	k_{10} (IL)	0.01	0; 0.01	0.028
	k_{11} (PL)	0.23	0.23; 0.24	<0.001
	k_{12} (SC)	−0.03	−0.03; −0.02	<0.001
	k_{13} ($SC^{0.5}$)	1.43	1.29; 1.57	<0.001
	k_{14} ($SC^{1/3}$)	−2.99	−3.28; −2.71	<0.001
Residential AB	k_0 (Intercept)	10.68	−2.72; 24.08	0.118
	k_1 (SR)	0.01	0; 0.02	0.035
	k_2 ($SR^{0.5}$)	−0.03	−0.05; −0.01	0.011
	k_3 (CR)	0.00	0; 0	<0.001
	k_4 ($CR^{0.5}$)	0.61	0.54; 0.68	<0.001
	k_5 ($CR^{1/3}$)	−2.50	−2.75; −2.24	<0.001
	k_6 (LPF)	4.81	0.56; 9.05	0.027
	k_7 ($LPF^{0.5}$)	−23.85	−41.75; −5.96	0.009
	k_8 ($LPF^{1/3}$)	22.74	6.51; 38.96	0.006
	k_9 (DL)	0.00	0; 0	0.106

Table A3. *Cont.*

Building Typology	Coefficient	Value	95% CI	*p*-Value
	k_{10} (IL)	0.00	−0.01; 0	0.164
	k_{11} (PL)	0.30	0.3; 0.3	<0.001
	k_{12} (SC)	−0.04	−0.04; −0.03	<0.001
	k_{13} ($SC^{0.5}$)	2.24	1.88; 2.6	<0.001
	k_{14} ($SC^{1/3}$)	−4.88	−5.67; −4.09	<0.001
Industrial	k_0 (Intercept)	17.96	4.47; 31.46	0.009
	k_1 (SR)	0.03	0.02; 0.05	<0.001
	k_2 ($SR^{0.5}$)	−0.06	−0.09; −0.03	<0.001
	k_3 (CR)	0.00	0; 0	<0.001
	k_4 ($CR^{0.5}$)	0.51	0.45; 0.58	<0.001
	k_5 ($CR^{1/3}$)	−2.12	−2.38; −1.87	<0.001
	k_6 (LPF)	−15.37	−19.02; −11.73	<0.001
	k_7 ($LPF^{0.5}$)	66.58	48.73; 84.44	<0.001
	k_8 ($LPF^{1/3}$)	−60.91	−77.94; −43.87	<0.001
	k_9 (DL)	−0.01	−0.01; −0.01	<0.001
	k_{10} (IL)	−0.01	−0.02; 0	0.010
	k_{11} (PL)	0.27	0.27; 0.27	<0.001
	k_{12} (SC)	0.01	0.01; 0.01	<0.001
	k_{13} ($SC^{0.5}$)	−0.31	−0.39; −0.24	<0.001
	k_{14} ($SC^{1/3}$)	0.54	0.4; 0.67	<0.001
Tertiary	k_0 (Intercept)	3.37	−10.24; 16.97	0.628
	k_1 (SR)	0.00	0; 0	0.737
	k_2 ($SR^{0.5}$)	0.00	−0.01; 0.01	0.935
	k_3 (CR)	0.00	0; 0	<0.001
	k_4 ($CR^{0.5}$)	0.42	0.38; 0.46	<0.001
	k_5 ($CR^{1/3}$)	−1.78	−1.94; −1.62	<0.001
	k_6 (LPF)	7.28	2.73; 11.82	0.002
	k_7 ($LPF^{0.5}$)	−37.45	−59.16; −15.75	0.001
	k_8 ($LPF^{1/3}$)	36.17	15.63; 56.71	0.001
	k_9 (DL)	0.00	0; 0	0.261
	k_{10} (IL)	−0.02	−0.03; −0.02	<0.001
	k_{11} (PL)	0.25	0.25; 0.25	<0.001
	k_{12} (SC)	−0.01	−0.01; −0.01	<0.001
	k_{13} ($SC^{0.5}$)	0.45	0.34; 0.57	<0.001
	k_{14} ($SC^{1/3}$)	−0.96	−1.21; −0.71	<0.001

Table A4. *QR* coefficients to estimate *PB* for each building typology.

Building Typology	Coefficient	Value	95% CI	*p*-Value
-	k_0 (Intercept)	0.22	0.21; 0.22	<0.001
Residential SFH	k_1 (IRR)	1.60	1.49; 1.7	<0.001
	k_2 (IRR^3)	−1.80	−2.74; −0.86	<0.001
	k_3 (IRR^3)	1.46	−0.63; 3.54	0.171
Residential TH	k_1 (IRR)	1.56	1.54; 1.59	<0.001
	k_2 (IRR^3)	−1.40	−1.57; −1.23	<0.001
	k_3 (IRR^3)	0.74	0.43; 1.06	<0.001
Residential MFH	k_1 (IRR)	1.55	1.53; 1.57	<0.001
	k_2 (IRR^3)	−1.47	−1.57; −1.37	<0.001
	k_3 (IRR^3)	0.90	0.74; 1.06	<0.001
Residential AB	k_1 (IRR)	1.55	1.53; 1.57	<0.001
	k_2 (IRR^3)	−1.49	−1.58; −1.39	<0.001
	k_3 (IRR^3)	0.88	0.75; 1	<0.001

Table A4. *Cont.*

Building Typology	Coefficient	Value	95% CI	*p*-Value
Industrial	k_1 (IRR)	1.54	1.53; 1.56	<0.001
	k_2 (IRR^3)	−1.40	−1.47; −1.34	<0.001
	k_3 (IRR^3)	0.76	0.67; 0.85	<0.001
Tertiary	k_1 (IRR)	1.56	1.55; 1.58	<0.001
	k_2 (IRR^3)	−1.48	−1.54; −1.43	<0.001
	k_3 (IRR^3)	0.84	0.77; 0.91	<0.001

References

1. SolarPower Europe. *EU Market Outlook For Solar Power 2022–2026*; SolarPower Europe: Brussels, Belgium, 2022; Available online: https://api.solarpowereurope.org/uploads/5222_SPE_EMO_2022_full_report_ver_03_1_319d70ca42.pdf (accessed on 26 February 2023).
2. IRENA. *Renewable Power Generation Costs in 2020*; IRENA: Abu Dhabi, United Arab Emirates, 2021.
3. Bórawski, P.; Holden, L.; Bełdycka-Bórawska, A. Perspectives of Photovoltaic Energy Market Development in the European Union. *Energy* **2023**, *270*, 126804. [CrossRef]
4. European Commission. *"Fit for 55": Delivering the EU's 2030 Climate Target on the Way to Climate Neutrality*; European Commission: Brussels, Belgium, 2021.
5. European Climate Foundation. *Building Europe's Net-Zero Future Why the Transition to Energy Efficient and Electrified Buildings Strengthens Europe's Economy*; European Climate Foundation: The Hague, The Netherlands, 2022.
6. Sun, L.; Chang, Y.; Wu, Y.; Sun, Y.; Su, D. Potential Estimation of Rooftop Photovoltaic with the Spatialization of Energy Self-Sufficiency in Urban Areas. *Energy Rep.* **2022**, *8*, 3982–3994. [CrossRef]
7. Matute, G.; Yusta, J.M.; Beyza, J.; Monteiro, C. Optimal Dispatch Model for PV-Electrolysis Plants in Self-Consumption Regime to Produce Green Hydrogen: A Spanish Case Study. *Int. J. Hydrog. Energy* **2022**, *47*, 25202–25213. [CrossRef]
8. Talavera, D.L.; Muñoz-Rodriguez, F.J.; Jimenez-Castillo, G.; Rus-Casas, C. A New Approach to Sizing the Photovoltaic Generator in Self-Consumption Systems Based on Cost—Competitiveness, Maximizing Direct Self-Consumption. *Renew. Energy* **2019**, *130*, 1021–1035. [CrossRef]
9. Hamann, K.R.S.; Bertel, M.P.; Ryszawska, B.; Lurger, B.; Szymański, P.; Rozwadowska, M.; Goedkoop, F.; Jans, L.; Perlaviciute, G.; Masson, T.; et al. An Interdisciplinary Understanding of Energy Citizenship: Integrating Psychological, Legal, and Economic Perspectives on a Citizen-Centred Sustainable Energy Transition. *Energy Res. Soc. Sci.* **2023**, *97*, 102959. [CrossRef]
10. Gassar, A.A.A.; Cha, S.H. Review of Geographic Information Systems-Based Rooftop Solar Photovoltaic Potential Estimation Approaches at Urban Scales. *Appl. Energy* **2021**, *291*, 116817. [CrossRef]
11. Sredenšek, K.; Štumberger, B.; Hadžiselimović, M.; Mavsar, P.; Seme, S. Physical, Geographical, Technical, and Economic Potential for the Optimal Configuration of Photovoltaic Systems Using a Digital Surface Model and Optimization Method. *Energy* **2022**, *242*, 122971. [CrossRef]
12. Gómez-Navarro, T.; Brazzini, T.; Alfonso-Solar, D.; Vargas-Salgado, C. Analysis of the Potential for PV Rooftop Prosumer Production: Technical, Economic and Environmental Assessment for the City of Valencia (Spain). *Renew. Energy* **2021**, *174*, 372–381. [CrossRef]
13. Han, J.Y.; Chen, Y.C.; Li, S.Y. Utilising High-Fidelity 3D Building Model for Analysing the Rooftop Solar Photovoltaic Potential in Urban Areas. *Sol. Energy* **2022**, *235*, 187–199. [CrossRef]
14. Fakhraian, E.; Alier, M.; Dalmau, F.V.; Nameni, A.; Guerrero, J.C. The Urban Rooftop Photovoltaic Potential Determination. *Sustainability* **2021**, *13*, 7447. [CrossRef]
15. Fakhraian, E.; Forment, M.A.; Dalmau, F.V.; Nameni, A.; Guerrero, M.J.C. Determination of the Urban Rooftop Photovoltaic Potential: A State of the Art. *Energy Rep.* **2021**, *7*, 176–185. [CrossRef]
16. Thebault, M.; Desthieux, G.; Castello, R.; Berrah, L. Large-Scale Evaluation of the Suitability of Buildings for Photovoltaic Integration: Case Study in Greater Geneva. *Appl. Energy* **2022**, *316*, 119127. [CrossRef]
17. Krapf, S.; Kemmerzell, N.; Uddin, S.K.H.; Vázquez, M.H.; Netzler, F.; Lienkamp, M. Towards Scalable Economic Photovoltaic Potential Analysis Using Aerial Images and Deep Learning. *Energies* **2021**, *14*, 3800. [CrossRef]
18. Fath, K.; Stengel, J.; Sprenger, W.; Wilson, H.R.; Schultmann, F.; Kuhn, T.E. A Method for Predicting the Economic Potential of (Building-Integrated) Photovoltaics in Urban Areas Based on Hourly Radiance Simulations. *Sol. Energy* **2015**, *116*, 357–370. [CrossRef]
19. Mansouri Kouhestani, F.; Byrne, J.; Johnson, D.; Spencer, L.; Hazendonk, P.; Brown, B. Evaluating Solar Energy Technical and Economic Potential on Rooftops in an Urban Setting: The City of Lethbridge, Canada. *Int. J. Energy Environ. Eng.* **2019**, *10*, 13–32. [CrossRef]
20. Wang, P.; Yu, P.; Huang, L.; Zhang, Y. An Integrated Technical, Economic, and Environmental Framework for Evaluating the Rooftop Photovoltaic Potential of Old Residential Buildings. *J. Environ. Manag.* **2022**, *317*, 115296. [CrossRef]

21. Olivella, J.; Domenech, B.; Calleja, G. Potential of Implementation of Residential Photovoltaics at City Level: The Case of London. *Renew. Energy* **2021**, *180*, 577–585. [CrossRef]
22. Ordóñez, Á.; Sánchez, E.; Rozas, L.; García, R.; Parra-Domínguez, J. Net-Metering and Net-Billing in Photovoltaic Self-Consumption: The Cases of Ecuador and Spain. *Sustain. Energy Technol. Assess.* **2022**, *53*, 102434. [CrossRef]
23. Vargas-Salgado, C.; Aparisi-Cerdá, I.; Alfonso-Solar, D.; Gómez-Navarro, T. Can Photovoltaic Systems Be Profitable in Urban Areas? Analysis of Regulation Scenarios for Four Cases in Valencia City (Spain). *Sol. Energy* **2022**, *233*, 461–477. [CrossRef]
24. Calcabrini, A.; Ziar, H.; Isabella, O.; Zeman, M. A Simplified Skyline-Based Method for Estimating the Annual Solar Energy Potential in Urban Environments. *Nat. Energy* **2019**, *4*, 206–215. [CrossRef]
25. Poon, K.H.; Kämpf, J.H.; Tay, S.E.R.; Wong, N.H.; Reindl, T.G. Parametric Study of URBAN Morphology on Building Solar Energy Potential in Singapore Context. *Urban Clim.* **2020**, *33*, 100624. [CrossRef]
26. Assouline, D.; Mohajeri, N.; Scartezzini, J.L. Large-Scale Rooftop Solar Photovoltaic Technical Potential Estimation Using Random Forests. *Appl. Energy* **2018**, *217*, 189–211. [CrossRef]
27. Mora-López, L.; Sidrach-De-Cardona, M. Models for the Optimization and Evaluation of Photovoltaic Self-Consumption Facilities. In Proceedings of the ISES Solar World Congress 2019, IEA SHC International Conference on Solar Heating and Cooling for Buildings and Industry 2019, Santiago, Chile, 4–7 November 2019; pp. 1555–1562. [CrossRef]
28. Fuster-Palop, E.; Prades-Gil, C.; Masip, X.; Viana-Fons, J.D.; Payá, J. Innovative Regression-Based Methodology to Assess the Techno-Economic Performance of Photovoltaic Installations in Urban Areas. *Renew. Sustain. Energy Rev.* **2021**, *149*, 111357. [CrossRef]
29. Varo-Martínez, M.; Fernández-Ahumada, L.M.; López-Luque, R.; Ramírez-Faz, J. Simulation of Self-Consumption Photovoltaic Installations: Profitability Thresholds. *Appl. Sci.* **2021**, *11*, 6517. [CrossRef]
30. Generalitat Valenciana Fichas Municipal Catarroja—Portal Estadístico de La Generalitat Valenciana—Generalitat Valenciana. Available online: https://pegv.gva.es/auto/scpd/web/FICHAS/Fichas/46094.pdf (accessed on 19 February 2023).
31. European Commission JRC Photovoltaic Geographical Information System (PVGIS). Available online: https://re.jrc.ec.europa.eu/pvg_tools/es/ (accessed on 15 February 2023).
32. Weather Similarity. Available online: https://www.codeminders.com/weather_similarity/ (accessed on 27 February 2023).
33. Dirección General del Catastro Sede Electrónica Del Catastro—Difusión de Datos Catastrales. Available online: https://www.sedecatastro.gob.es/Accesos/SECAccDescargaDatos.aspx (accessed on 14 February 2023).
34. Loga, T.; Diefenbach, N.; Balaras, C.A.; Droutsa, K.; Kontoyiannidis, S.; Zavrl, M.Š.; Rakušček, A.; Corrado, V.; Roarty, C.; Amtmann, M.; et al. *Typology Approach for Building Stock Energy Assessment. Main Results of the TABULA Project*; Institut Wohnen und Umwelt GmbH: Darmstadt, Germany, 2012.
35. Neuhäuser, M. Wilcoxon-Mann-Whitney Test. In *International Encyclopedia of Statistical Science*; Springer: Berlin/Heidelberg, Germany, 2011; pp. 1656–1658. [CrossRef]
36. Centro Nacional de Información Geográfica Centro de Descargas Del CNIG. Available online: http://centrodedescargas.cnig.es/CentroDescargas/buscadorCatalogo.do?codFamilia=LIDAR (accessed on 14 February 2023).
37. Biljecki, F.; Ledoux, H.; Stoter, J. An Improved LOD Specification for 3D Building Models. *Comput. Environ. Urban Syst.* **2016**, *59*, 25–37. [CrossRef]
38. Masip, X.; Fuster-Palop, E.; Prades-Gil, C.; Viana-Fons, J.D.; Payá, J.; Navarro-Peris, E. Case Study of Electric and DHW Energy Communities in a Mediterranean District. *Renew. Sustain. Energy Rev.* **2023**, *178*, 113234. [CrossRef]
39. Liu, B.Y.H.; Jordan, R.C. The Interrelationship and Characteristic Distribution of Direct, Diffuse and Total Solar Radiation. *Sol. Energy* **1960**, *4*, 1–19. [CrossRef]
40. Memme, S.; Fossa, M. Maximum Energy Yield of PV Surfaces in France and Italy from Climate Based Equations for Optimum Tilt at Different Azimuth Angles. *Renew. Energy* **2022**, *200*, 845–866. [CrossRef]
41. Liu, Z.; Liu, X.; Zhang, H.; Yan, D. Integrated Physical Approach to Assessing Urban-Scale Building Photovoltaic Potential at High Spatiotemporal Resolution. *J. Clean. Prod.* **2023**, *388*, 135979. [CrossRef]
42. Viana-Fons, J.D.; Gonzálvez-Maciá, J.; Payá-Herrero, J. Methodology for the Calculation of the Shadow Factor on Roofs and Facades of Buildings in Urban Areas. In Proceedings of the XI National and II International Engineering Thermodynamics Congress, Albacete, Spain, 12–14 June 2019; p. 29147.
43. Viana-Fons, J.D.; Gonzálvez-Maciá, J.; Payá, J. Development and Validation in a 2D-GIS Environment of a 3D Shadow Cast Vector-Based Model on Arbitrarily Orientated and Tilted Surfaces. *Energy Build.* **2020**, *224*, 110258. [CrossRef]
44. Fuster-Palop, E.; Vargas-Salgado, C.; Ferri-Revert, J.C.; Payá, J. Performance Analysis and Modelling of a 50 MW Grid-Connected Photovoltaic Plant in Spain after 12 Years of Operation. *Renew. Sustain. Energy Rev.* **2022**, *170*, 112968. [CrossRef]
45. Mehta, P.; Tiefenbeck, V. Solar PV Sharing in Urban Energy Communities: Impact of Community Configurations on Profitability, Autonomy and the Electric Grid. *Sustain. Cities Soc.* **2022**, *87*, 104178. [CrossRef]
46. Datadis. Available online: https://datadis.es/home (accessed on 15 February 2023).
47. Mor, G.; Cipriano, J.; Martirano, G.; Pignatelli, F.; Lodi, C.; Lazzari, F.; Grillone, B.; Chemisana, D. A Data-Driven Method for Unsupervised Electricity Consumption Characterisation at the District Level and Beyond. *Energy Rep.* **2021**, *7*, 5667–5684. [CrossRef]

48. Instituto Nacional de Estadística INEbase/Demografía y Población/Cifras de Población y Censos Demográficos/Censos de Población y Viviendas. 2011. Available online: https://www.ine.es/censos2011_datos/cen11_datos_inicio.htm (accessed on 21 September 2022).
49. Manso-Burgos, A.; Ribó-Pérez, D.; Gómez-Navarro, T.; Alcázar-Ortega, M. Local Energy Communities Modelling and Optimisation Considering Storage, Demand Configuration and Sharing Strategies: A Case Study in Valencia (Spain). *Energy Rep.* **2022**, *8*, 10395–10408. [CrossRef]
50. *MTE RD 244/2019*; Regulacion Condiciones Técnicas, Administrativas y Económicas Del Autoonsumo de Energía Eléctrica. Boletín Oficial del Estado: Madrid, Spain, 2019; pp. 35674–35719.
51. Comisión Nacional de los Mercados y la Competencia. *Circular 3/2020, de 15 de Enero, de La Comisión Nacional de Los Mercados y La Competencia, Por La Que Se Establece La Metodología Para El Cálculo de Los Peajes de Transporte y Distribución de Electricidad*; Comisión Nacional de los Mercados y la Competencia: Madrid, Spain, 2020.
52. Red Eléctrica de España Analysis—ESIOS Electricity. Available online: https://www.esios.ree.es/en/analysis/1739?vis=1&start_date=01-06-2021T00%3A00&end_date=01-06-2022T23%3A55&compare_start_date=31-05-2021T00%3A00&groupby=hour&compare_indicators=1739,1003,1004,1005 (accessed on 18 February 2023).
53. Som Energia Histórico de Tarifas de Electricidad. Available online: https://www.somenergia.coop/es/tarifas-de-electricidad/historico-de-tarifas-de-electricidad/ (accessed on 18 February 2023).
54. Manso-Burgos, Á.; Ribó-Pérez, D.; Alcázar-Ortega, M.; Gómez-Navarro, T. Local Energy Communities in Spain: Economic Implications of the New Tariff and Variable Coefficients. *Sustainability* **2021**, *13*, 10555. [CrossRef]
55. Instituto Valenciano de Competitividad Empresarial. *Resolución de 24 de Marzo de 2022, Del Presidente Del Instituto Valenciano de Competitividad Empresarial (IVACE), Por La Que Se Convocan Ayudas Destinadas Al Fomento de Instalaciones de Autoconsumo de Energía Eléctrica En Los Municipios de La Comunitat Va*; Instituto Valenciano de Competitividad Empresarial: Valencia, Spain, 2022.
56. Optimize Function—RDocumentation. Available online: https://www.rdocumentation.org/packages/stats/versions/3.6.2/topics/optimize (accessed on 25 February 2023).
57. Brent, R.P. *Algorithms for Minimization without Derivatives*; Courier Corporation: San Francisco, CA, USA, 2002; p. 195.
58. Simoiu, M.S.; Fagarasan, I.; Ploix, S.; Calofir, V. Optimising the Self-Consumption and Self-Sufficiency: A Novel Approach for Adequately Sizing a Photovoltaic Plant with Application to a Metropolitan Station. *J. Clean. Prod.* **2021**, *327*, 129399. [CrossRef]
59. Mansó Borràs, I.; Neves, D.; Gomes, R. Using Urban Building Energy Modeling Data to Assess Energy Communities' Potential. *Energy Build.* **2023**, *282*, 112791. [CrossRef]
60. Ciocia, A.; Amato, A.; Di Leo, P.; Fichera, S.; Malgaroli, G.; Spertino, F.; Tzanova, S. Self-Consumption and Self-Sufficiency in Photovoltaic Systems: Effect of Grid Limitation and Storage Installation. *Energies* **2021**, *14*, 1591. [CrossRef]
61. Beck, T.; Kondziella, H.; Huard, G.; Bruckner, T. Assessing the Influence of the Temporal Resolution of Electrical Load and PV Generation Profiles on Self-Consumption and Sizing of PV-Battery Systems. *Appl. Energy* **2016**, *173*, 331–342. [CrossRef]
62. Gallego-Castillo, C.; Heleno, M.; Victoria, M. Self-Consumption for Energy Communities in Spain: A Regional Analysis under the New Legal Framework. *Energy Policy* **2021**, *150*, 112144. [CrossRef]
63. Gilman, P.; Dobos, A.; Diorio, N.; Freeman, J.; Janzou, S.; Ryberg, D. *SAM Photovoltaic Model Technical Reference Update*; National Renewable Energy Laboratory (NREL): Golden, CO, USA, 2016.
64. Perpiñán, O. *Energía Solar Fotovoltaica*; Madrid, Spain. 2023. Available online: https://oscarperpinan.github.io/esf/ESF.pdf (accessed on 26 February 2023).
65. JA SOLAR JAM60S20 365–390 Datasheet. Available online: https://www.jasolar.com/uploadfile/2020/0619/20200619041705631.pdf (accessed on 18 February 2023).
66. Fu, R.; Feldman, D.; Margolis, R.U.S. *Solar Photovoltaic System Cost Benchmark: Q1 2018*; National Renewable Energy Laboratory (NREL): Golden, CO, USA, 2018.
67. Eurostat HICP—Annual Data (Average Index and Rate of Change). Available online: https://ec.europa.eu/eurostat/databrowser/view/prc_hicp_aind/default/table?lang=en (accessed on 19 February 2023).
68. Domenech, B.; Calleja, G.; Olivella, J. Residential Photovoltaic Profitability with Storage under the New Spanish Regulation: A Multi-Scenario Analysis. *Energies* **2021**, *14*, 1987. [CrossRef]
69. Agencia Tributaria Tax Agency: VAT Tax Rates. Available online: https://sede.agenciatributaria.gob.es/Sede/en_gb/iva/calculo-iva-repercutido-clientes/tipos-impositivos-iva.html (accessed on 19 February 2023).
70. Red Eléctrica de España REData—Non Renewable Detail CO2 Emissions | Red Eléctrica. Available online: https://www.ree.es/en/datos/generation/non-renewable-detail-CO2-emissions (accessed on 19 February 2023).
71. Prol, J.L.; Steininger, K.W. Photovoltaic Self-Consumption Is Now Profitable in Spain: Effects of the New Regulation on Prosumers' Internal Rate of Return. *Energy Policy* **2020**, *146*, 111793. [CrossRef]
72. Talayero, A.P.; Melero, J.J.; Llombart, A.; Yürüşen, N.Y. Machine Learning Models for the Estimation of the Production of Large Utility-Scale Photovoltaic Plants. *Sol. Energy* **2023**, *254*, 88–101. [CrossRef]
73. Huang, S. Linear Regression Analysis. In *International Encyclopedia of Education*, 4th ed.; Elsevier: Amsterdam, The Netherlands, 2023; pp. 548–557. [CrossRef]
74. Koenker, R. *Quantile Regression*; Cambridge University Press: Cambridge, UK, 2005; pp. 1–349. [CrossRef]
75. Hao, L.; Naiman, D.Q. *Quantile Regression*; SAGE Publications: Thousand Oaks, CA, USA, 2007; Volume 149, ISBN 978-1-4129-2628-7.

76. Koenker, R. CRAN—Package Quantreg. Available online: https://cran.r-project.org/web/packages/quantreg/ (accessed on 17 February 2023).
77. Box, G.E.P.; Cox, D.R. An Analysis of Transformations. *J. R. Stat. Soc. Ser. B* **1964**, *26*, 211–243. [CrossRef]
78. Sheather, S.J. Diagnostics and Transformations for Multiple Linear Regression. In *A Modern Approach to Regression with R.*; Springer: Berlin/Heidelberg, Germany, 2009; pp. 151–225. [CrossRef]
79. Ripley, B. *R Package MASS, Version 7.3–58.2; Support Functions and Datasets for Venables and Ripley's MASS*; R Foundation for Statistical Computing: Vienna, Austria, 2023.